

**A STUDY OF THE CORROSION RESISTANCE OF
GAMMA TITANIUM ALUMINIDE IN RINGER'S
SOLUTION, 3.5 WT% NaCl AND SEAWATER**

by

Carolina Delgado Alvarado

A thesis submitted in partial fulfillment of the requirements for the degree of

MASTER OF SCIENCE

In

MECHANICAL ENGINEERING

UNIVERSITY OF PUERTO RICO
MAYAGÜEZ CAMPUS
2005

Approved by:

Néstor L. Pérez, Ph.D.
Member, Graduate Committee

Date

Oscar Marcelo Suárez, Ph.D.
Member, Graduate Committee

Date

Paul A. Sundaram, Ph.D.
President, Graduate Committee

Date

Jose A. Colucci
Representative of Graduate Studies

Date

Paul A. Sundaram, Ph.D.
Chairperson of the Department

Date

ABSTRACT

Corrosion resistance is one of the essential requirements that determine the application of a metallic alloy as a biomaterial. The titanium alloy, gamma titanium aluminide (γ -TiAl), widely known for its low density, high strength-to-weight ratio, high stiffness, and strength was evaluated for room temperature corrosion resistance in this research to determine its viability as a biomaterial. For this purpose two fundamental electrochemical techniques namely Electrochemical Impedance Spectroscopy (EIS) and Potentiodynamic Anodic Polarization (PAP). were used to evaluate the corrosion performance of γ -TiAl, in Ringer's solution, 3.5% NaCl, and seawater. Ti-6Al-4V alloy, a popular biomaterial, was used as comparison. Surface modification treatments were employed with the purpose of improving corrosion resistance. The samples were oxidized at 500°C, 800°C, and autoclaved at 121°C and 15 psi. A scanning electron microscope (SEM) and X-ray diffraction (XRD) were used to characterize the samples. In general, the results of the potentiodynamic anodic polarization were found to be in good agreement with those of EIS analyses. The results obtained for γ -TiAl and Ti-6Al-4V were very similar. The presence of the oxide layer formed with the surface treatments increased their corrosion resistance. The low values of corrosion rate (C_R), and the high values for corrosion potential (E_{corr}) and polarization resistance (R_p) obtained experimentally implies that γ -TiAl can be competitively considered as an alternative metallic biomaterial.

RESUMEN

La resistencia a la corrosión es uno de los requerimientos esenciales que determinan la aplicación de una aleación metálica como biomaterial. El gamma titanio aluminio (γ -TiAl) el cual es una aleación ampliamente conocida por su baja densidad, alta relación resistencia-peso y alta rigidez fue evaluada en la presente investigación por su resistencia a corrosión a temperatura ambiente. Para este propósito dos técnicas electroquímicas fundamentales, espectroscopia de impedancia y polarización anódica potenciodinámica fueron utilizadas para evaluar a γ -TiAl en solución de Ringer, 3.5% NaCl y agua de mar. Ti-6Al-4V, uno de los biomateriales más comunes en la actualidad, fue evaluado como material de comparación. Con el propósito de mejorar la resistencia a la corrosión de estas aleaciones tres tratamientos de modificación de superficie fueron realizados estos consisten de un proceso de oxidación a 500°C y 800°C y un autoclaveado a 121°C y 15 psi. Dos técnicas de caracterización fueron utilizadas para evaluar las aleaciones de titanio estas fueron microscopia electrónica de rastreo y difracción de rayos X. Los resultados obtenidos para γ -TiAl y Ti-6Al-4V fueron muy similares. Se mejoró la resistencia a la corrosión de las aleaciones debido a la presencia de una capa de óxido de titanio formada con los tratamientos superficiales. Adicionalmente, los bajos valores obtenidos experimentalmente de velocidad de corrosión (C_R) y los altos valores de potencial de corrosión (E_{corr}) y resistencia a la polarización (R_p) implican que se puede considerar competitivamente al γ -TiAl como un biomaterial alternativo.

Copyright

By means of this document I authorize the library of the University of Puerto Rico Mayaguez Campus, the full or partial copy of this thesis work exclusively as an aid for the use of research work..

Carolina Delgado Alvarado

Date

TO MY FAMILY.....

My father Alberto, my mother Zully, my brother
Felipe, my grandmother Olga, and the rest of my family,
whom all this time from the distance have been my guiding
light and spiritual support

AND TO MY LOVE....

MING, because without him I wouldn't
have made it

ACKNOWLEDGEMENTS

First from all, thanks to GOD for EVERYTHING... and the HOLY SPIRIT for illuminating me all the time.

During the past two years, many people were related with me in the professional and personal aspect, for that reason I wish to dedicate this section to recognize their support.

I want to start expressing a sincere acknowledgement to my advisor, Dr. Paul A. Sundaram, who with motivation and supervision guided me to finish this great step in my life. Special thanks to Dr. Jose Colucci, from chemical engineering department, for his support, guidance, and transmitted knowledge for the completion of my work and Dr. Marcelo Suarez for him motivation and example.

Special thanks, to Omaira Rivera of Biology department, Jose Almodovar of Physics department, and Edgar Perez from Hewlett Packard for their technical support. Many, many thanks to Zory, from the Mechanical Engineering department, for her unconditional service during all this time. Thanks to Jessamine Hernandez, Pedro Velazquez, Nilsa Paris and all the staff of the Mechanical Engineering department. Special thanks also to my friends Victor Pereles, Juan Esteban Cataño, and Monica Ospinal for their help and motivation. And all the other people that directly or indirectly were related with my studies and my work.

TABLE OF CONTENTS

ABSTRACT	II
RESUMEN	III
COPYRIGHT.....	IV
ACKNOWLEDGEMENTS.....	VI
TABLE OF CONTENTS.....	VII
LIST OF TABLES	IX
LIST OF FIGURES	X
1 INTRODUCTION	1
1.1 Objectives	5
2 LITERATURE REVIEW	6
2.1 Definition of corrosion.....	6
2.2 Corrosion resistant materials.....	7
2.3 Biomaterials	8
2.3.1 Definition	8
2.3.2 Properties of biomaterials	8
2.3.3 Materials currently use as biomaterials.....	9
2.3.3.1 Titanium and titanium alloys	9
2.3.3.1.1 γ -TiAl.....	12
2.3.3.1.2 Ti-6Al-4V	14
2.4 Corrosion tests for evaluation of titanium alloys.....	16
2.4.1 Electrochemical Impedance Spectroscopy	17
2.4.1.1 Theory	17
2.4.1.2 Equivalent circuit elements.....	19
2.4.1.3 Randles Cell	20
2.4.1.4 Impedance plots	22
2.4.1.4.1 The Nyquist Plot	22
2.4.1.4.1.1 Special cases	23
2.4.1.4.2 The Bode Plot	24
2.4.2 Potentiodynamic anodic polarization.....	26
2.5 RECENT LITERATURE	28
3 METHODOLOGY	37
3.1 Materials	38
3.2 Sample preparation	38
3.3 Pre-treatment.....	40
3.4 Sampling	40
3.5 Sample characterization	41
3.6 Evaluation by electrochemical methods	42
4 RESULTS AND DISCUSSION.....	47
4.1 Characterization	47

4.1.1	Materials	47
4.1.2	Pre-treatments	50
4.1.2.1	γ -TiAl.....	50
4.1.2.2	Ti-6Al-4V	54
4.1.3	Characterization of autoclaved samples.....	58
4.2	Evaluation by Electrochemical methods.....	60
4.2.1	Potentiodynamic anodic polarization (PAP).....	60
4.2.1.1	Effect of medium temperature	66
4.2.2	Electrochemical impedance spectroscopy (EIS).....	71
4.2.2.1	Equivalent circuit	83
4.2.2.2	Temperature effect evaluation	84
4.2.2.3	General results for γ -TiAl with EIS technique.....	85
4.2.2.4	General results for Ti-6Al-4V with EIS technique.....	86
4.2.2.5	Comparison between γ -TiAl and Ti-6Al-4V with EIS technique.....	87
5	CONCLUSIONS.....	90
6	RECOMMENDATIONS	92
7	BIBLIOGRAPHY.....	93

LIST OF TABLES

Table 2-1. Some biomaterial applications [10].....	10
Table 2-2. Titanium and titanium alloys for biomedical applications	11
Table 2-3. Typical mechanical properties of titanium alloys for bioapplications	12
Table 2-4. Some properties of γ -TiAl alloys.....	13
Table 2-5. Composition of Ti-6Al-4V	14
Table 2-6. Typical physical properties for Ti-6Al-4V.....	15
Table 2-7. Typical mechanical properties for Ti-6Al-4V	15
Table 2-8. ASTM norms for corrosion testing of biomaterials	16
Table 2-9. Some circuits elements	20
Table 2-10. ASTM norms used for corrosion testing	28
Table 3-1. Experimental matrix	43
Table 4-1. Corrosion parameters of γ -TiAl for all treatments	61
Table 4-2. Corrosion parameters of Ti-6Al-4V for all treatments.....	61
Table 4-3. Corrosion parameters of γ -TiAl for temperature effect.....	67
Table 4-4. Corrosion parameters of Ti-6Al-4V for temperature effect	67
Table 4-5. Activation energy values for control and autoclaved samples of γ -TiAl and Ti-6Al-4V	70
Table 4-6. Ac impedance parameters for γ -TiAl for all treatments	72
Table 4-7. Ac impedance parameters for Ti-6Al-4V for all treatments	72
Table 4-8. Ac impedance parameters for γ -TiAl for temperature effect	84
Table 4-9. Ac impedance parameters for Ti-6Al-4V for temperature effect.....	84

LIST OF FIGURES

Figure 2-1. Copper-Zinc cell.....	6
Figure 2-2. AC waveforms for an applied potential and a resulting current	18
Figure 2-3. Equivalent circuit for a single electrochemical cell	21
Figure 2-4. Equivalent circuit for a metal coated with a non-conductive film	21
Figure 2-5. Nyquist Plot for a simple electrochemical system	22
Figure 2-6. Nyquist Plot for a metal coated with a non-conductive film	23
Figure 2-7. Nyquist Plot for Warburg Impedance behavior	24
Figure 2-8. Bode Plot for a simple electrochemical system	25
Figure 2-9. Potentiodynamic polarization curve.....	27
Figure 3-1. Experimental methodology flow-chart	37
Figure 3-2. Mechanical grinding process.....	39
Figure 3-3. Ultrasonic cleaning process.....	39
Figure 3-4. Autoclaving process	40
Figure 3-5. Electrochemical cell (K-cell)	44
Figure 3-6. Experimental setup for corrosion measurements	46
Figure 3-7. Experimental setup for evaluation at different temperatures	46
Figure 4-1. Microstructure of γ -TiAl (a) optical image (b) backscattered electron image	48
Figure 4-2. Microstructure of Ti-6Al-4V (a) optical image (b) backscattered electron image.....	48
Figure 4-3. XRD pattern of as-received (control) sample of γ -TiAl	49
Figure 4-4. XRD pattern of as-received (control) sample of Ti-6Al-4V	49
Figure 4-5. Cross sectional SEM micrographs of γ -TiAl (P: polymeric resin, M: metal) (a) control sample, (b) autoclaved sample, (c) oxidation treatment at 500°C, (d) oxidation treatment at 800°C.....	52
Figure 4-6. XRD pattern after treatment of γ -TiAl (a) autoclaved sample,.....	53
Figure 4-7. Cross sectional SEM micrographs of Ti-6Al-4V (P: polymeric resin, M:metal) (a)control sample, (b) autoclaved sample, (c) oxidation treatment at 500°C, (d) oxidation treatment at 800°C.....	55
Figure 4-8. XRD pattern after treatment of Ti-6Al-4V (a) autoclaved sample,	57
Figure 4-9. Comparison between XRD patterns of γ -TiAl for the different autoclaving times.....	59
Figure 4-10. Comparison between XRD patterns of Ti-6Al-4V for the different autoclaving times	59
Figure 4-11. Potentiodynamic anodic polarization curves for Ti-6Al-4V after thermal treatment at 800°C	63
Figure 4-12. Potentiodynamic anodic polarization curves for Ti-6Al-4V control	64
Figure 4-13. Temperature effect in control samples of γ -TiAl	68
Figure 4-14. Temperature effect in control samples of Ti-6Al-4V	68
Figure 4-15. E_{corr} vs Temperature	69
Figure 4-16. I_{corr} vs Temperature.....	69
Figure 4-17. Corrosion rate vs Temperature.....	70

Figure 4-18. Arrhenius plot for γ -TiAl and Ti-6Al-4V control and autoclaved samples in Ringer's solution.....	71
Figure 4-19. Nyquist plot for γ -TiAl in 3.5% NaCl.....	76
Figure 4-20. Nyquist plot for γ -TiAl in Ringer's solution.....	76
Figure 4-21. Nyquist plot for γ -TiAl in seawater.....	77
Figure 4-22. Nyquist plot for Ti-6Al-4V in 3.5% NaCl	77
Figure 4-23. Nyquist plot for Ti-6Al-4V in Ringer's solution	78
Figure 4-24. Nyquist plot for Ti-6Al-4V in seawater	78
Figure 4-25. Bode Plots for γ -TiAl control in Ringer's solution (a) Bode Phase (b) Bode $ Z $	81
Figure 4-26. Bode Plots for in Ringer's solution for γ -TiAl at 500°C (a) Bode Phase (b) Bode $ Z $	81
Figure 4-27. Bode Plots for Ti-6Al-4V control in Ringer's solution (a) Bode Phase (b) Bode $ Z $	82
Figure 4-28. Bode Plots in Ringer's solution for Ti-6Al-4V oxidized at 800°C (a) Bode Phase (b) Bode $ Z $	82
Figure 4-29. Equivalent electrochemical circuits for γ -TiAl and Ti-6Al-4V (a) simple RCPE for control, autoclaved, and oxidized at 500°C (b) RCPE for oxidation treatment at 800°C.....	83
Figure 4-30. Temperature effect in control and autoclaved samples of γ -TiAl and Ti-6Al-4V with EIS technique.....	85
Figure 4-31. General behavior of γ -TiAl with EIS technique.....	86
Figure 4-32. General behavior of Ti-6Al-4V with EIS technique	87
Figure 4-33. Behavior of γ -TiAl and Ti-6Al-4V in 3.5% NaCl	88
Figure 4-34. Behavior of γ -TiAl and Ti-6Al-4V in Ringer's solution.....	88
Figure 4-35. Behavior of γ -TiAl and Ti-6Al-4V in seawater	89

1 INTRODUCTION

Determining the capacity of materials to resist deterioration without modifying their surface and bulk initial properties, when exposed to aggressive media during service, is one of the important pieces of information required at the moment of selecting a material for a given application. Corrosion science has guidelines on experiments and characterization techniques that determine whether a material can be considered as resistant to corrosion.

Corrosion is an electrochemical process. This is mainly a surface phenomenon that consists in a transfer of electrons from one chemical species to another, and determined by two principal reactions an anodic reaction where oxidation occurs and a cathodic reaction where reduction occurs. At the present time, a great diversity of metallic materials exist, such as stainless steels, cobalt-based alloys, chromium and nickel-based alloys, and titanium alloys, that are considered as materials which resist aggressive media in applications required at the engineering level. For example, these materials are used in the aerospace industry and, with a more direct human impact, as biomaterials.

In recent years, biomaterials have been considered as one of the areas of greatest impact at the research level. A biomaterial is a pharmacologically inert device, whose main function is to replace and/or to restore live tissue and its functions [1]. To be considered a biomaterial, the main characteristic of any material is its biocompatibility.

This means that the biomaterial must be accepted by the organism in which it is implanted without development of a negative response due to its presence. Additional requirements are that they must not be toxic or carcinogenic, but chemically stable (corrosion resistant in body fluids), mechanically resistant with an extended fatigue life, and have appropriate density [1]. Four types of biomaterials are generally used: metals, polymers, ceramics, and composites. There are a variety of clinical applications for polymeric biomaterials such as dentures, facial prosthesis, bones and joints, and knee joints where the most commonly used polymers are poly (methyl methacrylate) (PMMA), polyethylene, acrylic and silicone. The ceramics biomaterials are generally used to repair, or replace, skeletal hard connective tissues principally using hydroxyapatite or Al_2O_3 (polycrystalline). Reinforcing systems with carbon fibers, polymer fibers, ceramics, and glasses are some composite biomaterials. At the present time, the mainstay in implant technology are materials such as stainless steels, Co-Cr alloys and titanium/titanium-base alloy systems [2].

Titanium and some of its alloys are widely used as biomaterials for dental and orthopedic applications due to their excellent mechanical properties with a satisfactory corrosion behavior, the most common being commercially pure titanium and Ti-6Al-4V. More than 2.2 million titanium devices of different descriptions and functions are implanted in patients worldwide every year [3]. These materials are classified as biologically inert biomaterials, or bioinert. Furthermore, they do not induce allergic reactions, such as those observed occasionally with some stainless steels. Yet, for increased safety, they are often modified by coating them with hydroxyapatite (which

simulates a bone component). This provides a bioactive surface and promotes normal growth of the body tissues [4].

Titanium alloys have a strong affinity for oxygen due to their high titanium content and promote promoting the formation of a stable and tightly adherent protective oxide layer on their surface. This is the reason for the good corrosion properties of these materials. In biomedical applications, the chemical composition and stability of this surface oxide layer is very important because the surface of a biomaterial is in direct contact with biological tissues. Recently, some studies have shown that the possibility of vanadium release in Ti-6Al-4V, considered as a toxic element may give rise to biocompatibility problems, altering the stability of this alloy and its viability as a biomaterial [5,6]. Additionally, this alloy possess other disadvantage such as the loss of mechanical properties when it is in contact with soft connective tissues [1].

In light of the stringent requirements for a chemically stable implant material, corrosion resistance is one of the essential requirements that determine the application of a metallic alloy as a biomaterial. It is critical that its properties remain unchanged when implanted in the human body. Recently, the metallic alloy gamma titanium aluminide (γ -TiAl) has been evaluated as an implant material showing excellent tissue response [7]. This material is widely known for its low density, high strength-to-weight ratio, high stiffness, and strength and could be possibly considered as a substitute material to Ti-6Al-4V without vanadium for use in biomedical devices.

To consider the possible use of γ -TiAl as an implant material, its corrosion properties must be carefully evaluated in a body fluid environment. The purpose of this research is to propose γ -TiAl as a metallic biomaterial alternative to the broadly used Ti-6Al-4V, by specifically evaluating its corrosion resistance. For this purpose, Electrochemical Impedance Spectroscopy (EIS) and potentiodynamic anodic polarization (PAP), two common electrochemical techniques will be employed [8] and, as the electrolyte, Ringer's solution will be used [9], which simulates the conditions closest to the human body. As an addition to this study two other electrolytes 3.5% NaCl and seawater will be utilized since there are, common in material corrosion testing and evaluation. Finally, surface modification treatments will be made to generate a barrier on the alloy surface, which produces a surface oxide layer to improve the corrosion resistance of these alloys.

1.1 Objectives

The main objective of this research is to determine the corrosion resistance of γ -TiAl by means of Potentiodynamic Anodic Polarization (PAP) and Electrochemical Impedance Spectroscopy (EIS) to verify its viability as a metallic biomaterial.

The specific objectives are:

- Evaluate the corrosion behavior of γ -TiAl in different electrolytes, such as Ringer's solution, NaCl 3.5% and seawater.
- Evaluate Ti-6Al-4V as a biomaterial of comparison.
- Evaluate the corrosion resistance after surface modification of γ -TiAl and Ti-6Al-4V.
- Determine the temperature effect on the corrosion behavior of γ -TiAl and Ti-6Al-4V at ambient temperature (25°C) and human body temperature (37°C).
- Analyze the results and by means of material characterization methods, such as scanning electron microscopy (SEM) and x-ray diffraction (XRD), provide a possible corrosion mechanism for these materials in the different media.

2 LITERATURE REVIEW

2.1 Definition of corrosion

Corrosion is a deterioration or destruction of a metal by means of a chemical or electrochemical reaction with its environment. The corrosion process can be chemical if the material tries to return to its original state (lowest energy), or electrochemical due to a current flow that produces a chemical reaction where there is a loss and gain of electrons. Two reactions are involved in this process: anodic and cathodic. Examples of these reactions is shown below for a copper – zinc system (Figure 1) which is governed by the following equations:

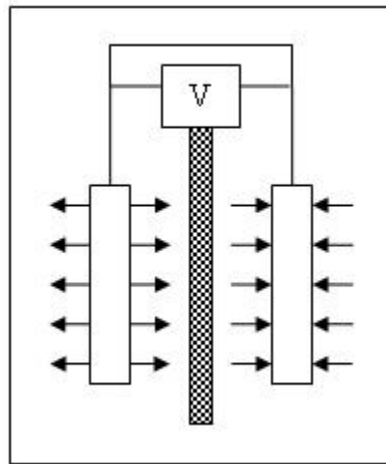
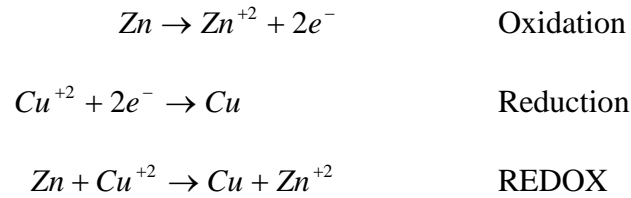


Figure 2-1. Copper-Zinc cell

In this system, zinc loses two electrons and copper gains the same number of electrons reducing ions. The resulting equation, called REDOX, represents the overall reaction at equilibrium where the anodic and cathodic reaction rates are equal.

It is possible to determine the different types of corrosion based on their appearance. Among these are general corrosion, galvanic corrosion, pitting corrosion, crevice corrosion, stress corrosion, biological corrosion, and others.

2.2 Corrosion resistant materials

Establishing the corrosion resistance for metallic alloys is very important to determine its viability for a particular application. Stainless steel is probably the most widely known and commonly used material of construction for corrosion resistance. For many years this was the only material available to provide any degree of resistance to corrosive attack. There are more than 70 standard categories of stainless steels. Many special alloys are classified into three main types: austenitic, martensitic and ferritic. Additionally, there exist a variety of materials resistant to corrosion such as nickel and high nickel alloys, copper and copper alloys, aluminum alloys, tantalum, zirconium, and the metallic material evaluated in this study, titanium alloys. Biomaterials have a very specific application in which corrosion resistance is of utmost importance due to its direct contact with living tissues and fluids in humans.

2.3 Biomaterials

2.3.1 Definition

A biomaterial is used as an inert device whose main purpose is to replace or restore function to a body tissue in direct contact with body fluids. This definition excludes materials used in surgical or dental applications and external prostheses, because in the former, although these instruments are exposed to body fluids, they do not replace the function of human tissue and, in the latter, they are not directly exposed to body fluids.

2.3.2 Properties of biomaterials

To be considered an “ideal” biomaterial there are three main requirements for a metallic material: biocompatibility, adequate mechanical properties, and ease of manufacturing.

The most important property required for a biomaterial is biocompatibility, which is related to tissue reactions, changes in properties (mechanical, physical, and chemical) and possibility of degradations in the material. Ductility, toughness, creep, and wear resistance are some mechanical properties required for a biomaterial, while fabrication methods, consistency, and conformity to all requirements and cost of product are manufacturing characteristics that finally determine the selectivity of a material.

Of these properties, biocompatibility is the closest related to this research due to the involved mechanism of interaction between the material and the tissue, the possibility of

ion or molecule release, and their mobility in the body, terms directly related with corrosion resistance.

2.3.3 Materials currently use as biomaterials

Currently, there are a variety of materials that can be recognized as biomaterials because they fulfill all requirements needed for such applications. These materials can be divided into the following categories: metals, polymers, ceramics and composites. Table 2.1, shows some materials and their respective medical and dental applications.

From these types of materials, two titanium alloys, namely gamma titanium aluminide (γ -TiAl) and Ti-6Al-4V (currently the most popular Ti-based biomaterial) will be evaluated.

2.3.3.1 Titanium and titanium alloys

Titanium, and its alloys, are commonly used as biomaterials due to excellent biocompatibility, with little or no reaction to surrounding tissue. Titanium has an extreme reactivity to oxygen and promotes the formation of a stable oxide film on its surface, thus giving it its corrosion resistance. These attractive properties, along with their low modulus of elasticity, were a driving force to the early introduction of some titanium alloys as biomaterials. Among these alloys were CP-Ti commercially pure titanium, the extra-low interstitial (ELI) Ti-6Al-4V alloy, and recently, the new titanium alloy compositions and metastable β alloys. Additionally, because of the problems

caused by other alloys due to vanadium release, Ti alloys without vanadium were developed; among these are $\alpha + \beta$ alloys: Ti-7Nb-6Al, Ti-13Nb-13Zr, and Ti-15Zr-4Nb.

Table 2.2 presents some titanium alloys developed for implant applications.

Table 2-1. Some biomaterial applications [10]

MATERIAL		APPLICATION
METALS AND ALLOYS	316L, stainless steel	Bone screws, total joint prostheses, wires
	Co-Cr-Mo, Co-Ni-Cr-W-Mo	Dental implants, bone and joint replacement, hip prostheses
	CP Ti, Ti-6Al-4V Ti-13Nb-13Zr	Dental implants, Orthopedic implants, bone and joint replacement
POLYMERS	Polymethyl methacrylate	Bone cement, artificial teeth, denture materials, intraocular lenses and hard contact lenses
	Polyethylene	Knee joints, connectors and bottles
	Polyster, silicone, PVC	Facial prostheses
	Silicones, PVC, nylon	Gastrointestinal segments, Finger joints
CERAMICS	Al ₂ O ₃ , hydroxylapatite	Orthopedic load-bearing applications, dental implants and Maxilofacial reconstruction
	Carbon fibers, calcium/phosphorus base glass fibers	Orthopedic fixation devices

Table 2-2. Titanium and titanium alloys for biomedical applications

TITANIUM ALLOY	TYPE
Pure titanium (ASTM F67)	Grade 1,2,3 and 4
Ti-6Al-4V ELI (ASTM F136)	$\alpha + \beta$
Ti-6Al-7Nb (ASTM F1295)	$\alpha + \beta$
Ti-5Al-2.5Fe (ISO/DIS 5832-10)	β rich and $\alpha + \beta$
Ti-5Al-3Mo-4Zr	$\alpha + \beta$
Ti-15Sn-4Nb-2Ta-0.2Pd	$\alpha + \beta$
Ti-15Zr-4Nb-2Ta-0.2Pd	$\alpha + \beta$
Ti-13Nb-13Zr	β
Ti-12Mo-6Zr-2Fe	β
Ti-15Mo	β
Ti-16Nb-10Hf	β
Ti-15Mo-5Zr-3Al	β
Ti-15Mo-3Nb	β
Ti-35.3Nb-5.1Ta-7.1Zr	β
Ti-29Nb-13Ta-4.6Zr	β

In addition to the mechanical properties such as fracture toughness, tensile strength, and fatigue, Table 2.3 shows mechanical properties for Ti alloys that are desirable in a biomaterial.

Table 2-3. Typical mechanical properties of titanium alloys for bioapplications

ALLOY	TENSILE STRENGTH (MPa)	YIELD STRENGTH (σ_y)	ELONGATION (%)	MODULUS (GPa)
Pure Ti grade 1	240	170	24	102.7
Pure Ti grade 2	345	275	20	102.7
Ti-6Al-4V (ELI)	860-965	795-875	10-15	101-110
Ti-6Al-7Nb	900-1050	880-950	8.1-15	114
Ti-5Al-2.5Fe	1020	895	15	112
Ti-5Al-1.5B	925-1080	820-930	15-17	110
Ti-15Sn-4Nb-2Ta-0.2Pd	860	790	21	89
Ti-13Nb-13Zr	973-1037	836-908	10-16	79-84
Ti-15Mo	874	544	21	78
Ti-15Mo-5Zr-3Al	852	838	25	80
Ti-35.3Nb-5.1Ta-7.1Zr	596.7	547.1	19	55
Ti-29Nb-13Ta-4.6Zr	911	864	13.2	80

2.3.3.1.1 γ -TiAl

γ -TiAl is an intermetallic material, commonly used in applications where high temperature is required. Compared to other materials, these alloys offer opportunities for substantial weight reductions, and compared to titanium alloys they offer better creep, oxidation and burn resistance, and increased strength at elevated temperatures. The γ -TiAl alloys commonly used are in the range Ti-(46-52)Al-(1-10)M, where M is at least one element from V, Cr, Mn, Nb, Ta, W and Mo. These alloys can be divided into single phase (γ) and two-phase ($\gamma + \alpha_2$) alloys. In the present research Ti-48Al-2Cr-2Nb alloy a two-phase alloy was studied.

With an appropriate thermo-mechanical processing, the microstructure of the phases can be adjusted to be either lamellar ($\gamma + \alpha_2$ and γ), platelet or equiaxed (gamma grains), or a

mixture of both morphologies. In these kinds of alloys, the ratio of lamellar to equiaxed γ must be controlled. A lamellar volume fraction of about 30% gives a reasonable combination of properties with good high-temperature creep resistance and acceptable tensile strength and ductility. This alloy has higher elastic modulus and lower density than Ti_3Al (α_2) alloys. However, at room temperature fracture resistance and ductility are considered “poor”. For that reason V, Mn, and Cr in small quantities (1-3%) are added to increase ductility while Nb, Ta, and Mn are added to improve strength and oxidation resistance. Table 2.4 shows some properties of γ -TiAl alloys.

Table 2-4. Some properties of γ -TiAl alloys

PROPERTY	VALUE
Density (g/cm^3)	3.7-3.9
Modulus (GPa)	130-140
Yield strength (MPa)	400-650
Tensile strength (MPa)	450-800
Ductility % at room temperature	4-1
Ductility % at high temperature	10-60
Fracture toughness ($\text{MPa (m)}^{1/2}$)	10-20
Creep limit ($^{\circ}\text{C}$)	1000
Oxidation ($^{\circ}\text{C}$)	900

Additionally, for low cycle fatigue, fine grain sizes increase fatigue life at temperatures lower than 800°C . Impact resistance and fracture toughness are low at room temperatures, but fracture toughness increases if the temperature increases and in the presence of higher proportions of the lamellar microstructure. In a two-phase quaternary γ alloy a fracture toughness of $12 \text{ MPa m}^{1/2}$ is observed for a fine structure which is almost completely γ and $K_{\text{IC}} > 20 \text{ MPa m}^{1/2}$ when a large volume fraction of lamellar

grains are present. Although, γ -TiAl alloy is currently using in aircraft and spacecraft applications, the purpose of this research is to improve its feasibility as biomaterial for other application.

2.3.3.1.2 Ti-6Al-4V

Ti-6Al-4V is one of the most commonly used titanium alloys. This is an alpha-beta alloy containing 6% Aluminum and 4% Vanadium. This alloy exhibits an excellent combination of corrosion resistance, strength, and toughness. Typical applications include medical devices, implants, aerospace applications, and pressure vessels. This kind of material complies with the ASTM F136 norm wich covers the chemical, mechanical, and metallurgical requirements for wrought annealed titanium-6aluminum-4vanadium ELI (extra low interstitial) alloy to be used in the manufacture of surgical implants. Table 2.5 shows the typical composition of Ti-6Al-4V.

Table 2-5. Composition of Ti-6Al-4V

ELEMENT	CONTENT
C	0.08%
Fe	0.25%
N ₂	0.05%
O ₂	0.20%
Al	5.5-6.76%
V	3.5-4.5%
Ti	Balance

The selection of this alloy as biomaterial is determined by a combination of most favorable characteristics including immunity to corrosion, bio-compatibility, strength,

low modulus and density and the capacity for integrating with bone and other tissue. The mechanical and physical properties of Ti-6Al-4V combine to provide implants, which are highly damage tolerant. Table 2.6 and 2.7 summarize the physical and mechanical properties of Ti-6Al-4V.

Table 2-6. Typical physical properties for Ti-6Al-4V

PROPERTY	TYPICAL VALUE
Density (g/cm ³)	4.42
Melting range (°C ± 15°C)	16.49
Specific heat (J/Kg.°C)	560
Volume electrical resistivity (Ω.cm)	170
Thermal conductivity (W/m.K)	7.2
Mean co-efficient of thermal expansion (0-100°C/°C)	8.6*10 ⁻⁶
Mean co-efficient of thermal expansion (0-300°C/°C)	9.2*10 ⁻⁶

Table 2-7. Typical mechanical properties for Ti-6Al-4V

PROPERTY	MINIMUM	TYPICAL VALUE
Tensile strength (MPa)	897	1000
0.2% Stress (MPa)	828	910
Elongation over 2 inches %	10	18
Reduction in area %	20	
Elastic modulus (GPa)		114
Hardness Rockwell C		36
Specific bend radius <0.070 in x thickness		4.5
Specific bend radius >0.070 in x thickness		5.0
Welded bend radius x thickness	6	
Charpy, V-Notch impact (J)		24

The microstructure of Ti-6Al-4V alloy depends upon heat treating and mechanical working. If the alloy is heated and worked at temperatures near but not exceeding the beta transus, and then annealed, a microstructure of fine-grained alpha with beta as a second phase at grain boundaries, such as the alloy evaluated in this research, can be produced. If the alloy is heated into the beta phase field (above 1000°C) and is then

cooled slowly to room temperature, two phases are obtained large beta grains and platelet alpha structure with grains. This kind of titanium alloy is widely used for total joint replacement arthroplasty (primarily hips and knees) application, in the orthopedic industry.

2.4 Corrosion tests for evaluation of titanium alloys

There are standardized tests developed to evaluate the corrosion behavior of implant materials/devices such as those presented in Table 2.8 [10].

In this research, two fundamental electrochemical techniques were used to evaluate the corrosion performance of γ -TiAl and Ti-6Al-4V, namely Electrochemical Impedance Spectroscopy (EIS) and Potentiodynamic Anodic Polarization (PAP).

Table 2-8. ASTM norms for corrosion testing of biomaterials

ASTM No.	Title
F746	Pitting or Crevice Corrosion of Metallic Surgical Implant Materials
F897	Fretting Corrosion of Osteosynthesis Plates and Screws
1801	Corrosion Fatigue Testing of Metallic Implant Materials
1814	Evaluating Modular Hip and Knee Joint Components
1875	Fretting Corrosion Testing of Modular Implant Interface: Hip Femoral Head-Bore and Cone Taper Interface

2.4.1 Electrochemical Impedance Spectroscopy

Electrochemical impedance spectroscopy (EIS) is an alternating current (ac) technique used for studying the spontaneous passivation of metals in electrolyte. It is a very useful tool to characterize an electrochemical system in terms of an equivalent electric circuit.

The EIS method offers three advantages over dc techniques: 1) small amplitude, using small excitations in the range of 5 to 10 mV peak to peak, causing minimal perturbation thus reducing errors, 2) allows study of mechanism, providing data on both electrodes about capacitance and charge transfer kinetics, and 3) measurement accuracy, measuring in low conductivity solutions due to the absence of a potential scan.

2.4.1.1 Theory

In alternating current (ac) the frequency is non-zero and the analogous equation to Ohm's Law is:

$$E = IZ$$

where E, I, and Z are the potential, current, and impedance, respectively. Resistors, capacitors, and inductors impede the flow of electrons in an AC circuit and can be considered analogous to diffusion, slow preceding chemical reactions and slow electrode kinetics in an electrochemical cell.

In this technique an AC voltage or current is applied over a wide range of frequencies and the current or voltage response of an electrochemical system is measured. If a sinusoidal potential excitation is applied, the response to this potential is an AC current at the same frequency but shifted in phase. Fig 2.2 shows this behavior.

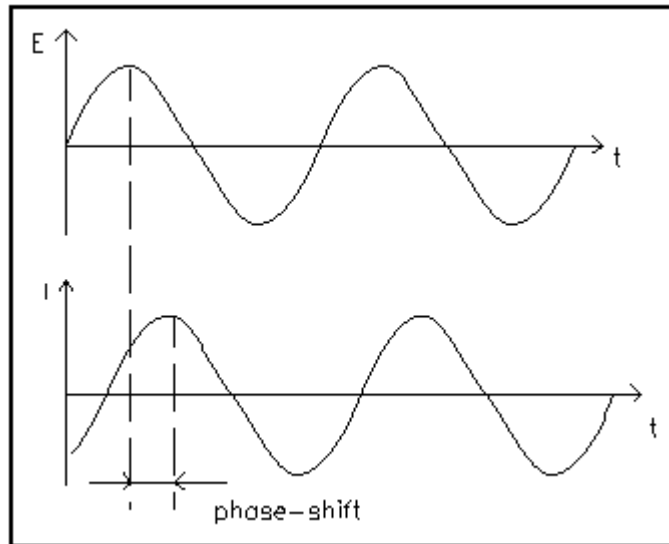


Figure 2-2. AC waveforms for an applied potential and a resulting current

The excitation signal, expressed as a function of time has the form:

$$E(t) = E_o \cos(\omega t)$$

Where $E(t)$, E_o , and ω are the potential at time t , amplitude of the signal, and the radial frequency, respectively. The response signal is represented by

$$I(t) = I_o \cos(\omega t + \phi)$$

The relationship between these expressions allows the calculation of the impedance of the system as:

$$Z = \frac{E(t)}{I(t)} = \frac{E_o \cos(\omega t)}{I_o \cos(\omega t + \phi)} = Z_o \frac{\cos(\omega t)}{\cos(\omega t + \phi)}$$

Impedance represents an opposition to the flow of electrons or current in an AC circuit due to the presence of resistors, capacitors, and inductors. Impedance can be expressed as a complex number where resistance is the real component and the combined capacitance and inductance is the imaginary component. This is expressed as:

$$Z_{total} = \frac{E' + E'' j}{I' + I'' j}$$

the resulting vector expression for the AC impedance will be:

$$Z_{total} = Z' + Z'' j$$

the absolute magnitude of the impedance is:

$$|Z| = \sqrt{Z'^2 + Z''^2}$$

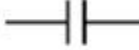
and the phase angle is defined by:

$$\tan \theta = \frac{Z''}{Z'}$$

2.4.1.2 Equivalent circuit elements

Electrochemical impedance spectroscopy is commonly analyzed by fitting it to an equivalent electrical circuit model. Table 2.9 shows the main circuit elements and their impedance equations.

Table 2-9. Some circuits elements

Circuit Element	Impedance Equation
	$Z = R + 0j$ $j = \sqrt{-1}$
	$Z = 0 - j / \omega C$ $\omega = 2\pi f$
	$Z = 0 + j \omega L$ $\omega = 2\pi f$

From Table 2.9 it can be concluded that:

- ✓ Impedance of a resistor is independent of frequency and only has a real component, for which reason the current through a resistor is always in phase with the voltage.
- ✓ The impedance of a capacitor decreases as the frequency increases. Capacitors only have an imaginary impedance component and the current through a capacitor is phase shifted -90 degrees with respect to the voltage.
- ✓ The impedance of an inductor is directly proportional to frequency. Inductors also have only an imaginary component and the inductor's current is phase shifted +90 degrees with respect to the voltage.

2.4.1.3 Randles Cell

The Randles cell is one of the most common cell models used to define electrochemical system. It includes a solution resistance between the working and reference electrodes (R_{Ω}), a charge transfer or polarization resistance at the electrode/solution interface (R_p),

and a double layer capacitor at this interface. The R_p component generally indicates the degree of film formation or the integrity of an organic coating. Figure 2.3 shows the equivalent circuit for the Randles cell. The double layer capacity is in parallel with the impedance due to the charge transfer reaction.

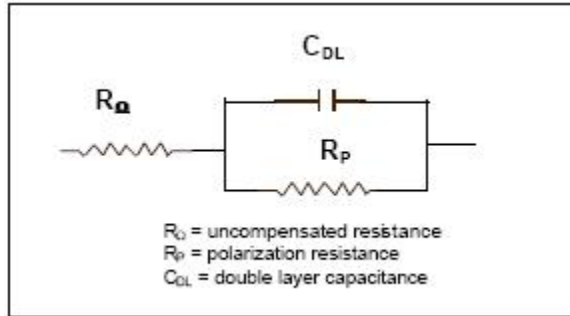


Figure 2-3. Equivalent circuit for a single electrochemical cell

If the material studied has a porous, non-conductive film on it, an equivalent circuit can be proposed (figure 2.4). The additional circuit elements are the coating capacitance (C_c) and the pore resistance (R_c).

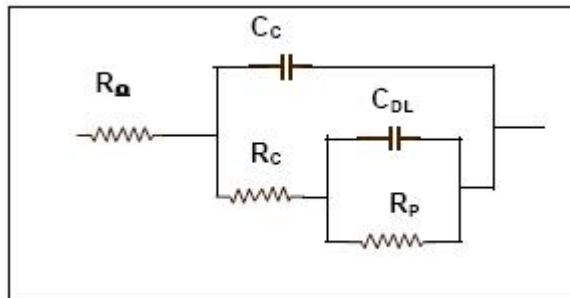


Figure 2-4. Equivalent circuit for a metal coated with a non-conductive film

2.4.1.4 Impedance plots

There are two principal impedance plot types to represent the experimental data obtained over a range of frequencies for an electrochemical system: Nyquist Plot and Bode Plot, both can show the true behavior of a real chemical system.

2.4.1.4.1 The Nyquist Plot

The Nyquist plot is a common format to evaluate electrochemical impedance data. It is obtained by plotting the real part of the impedance on the X axis and the imaginary part on the Y axis at each excitation frequency. Figure 2.5 shows a typical Nyquist plot expected for the simple circuit shown in figure 2.3

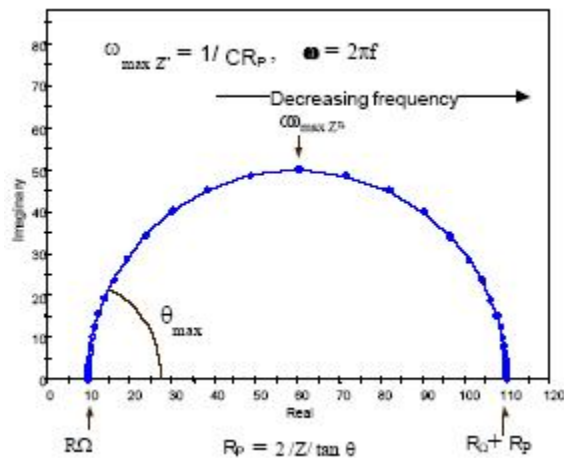


Figure 2-5. Nyquist Plot for a simple electrochemical system

The Nyquist plot has a range from high frequencies to low frequencies. At high frequencies, the impedance of the Randless Cell is almost created by the ohmic resistance, R_{Ω} , while at low frequencies it is approximated by a pure resistance, R_p . These values can be read directly for the Nyquist Plot and if the frequency corresponding

to the top of the semicircle, ω ($\theta = \max$), is known it is possible to calculate the capacitance using the following expression:

$$C = \frac{1}{\omega_{\max} R_p} = \frac{1}{2\pi f R_p}$$

2.4.1.4.1.1 Special cases

Coated Metal

If a material has a non-conductive film on its surface like the one presented in Figure 2.4, the corresponding Nyquist Plot reveals the presence of two semicircles, one smaller than the other as shown in fig 2.6 and it is possible to calculate R_{Ω} , C_C , R_C , C_{DL} and R_p directly from the graph.

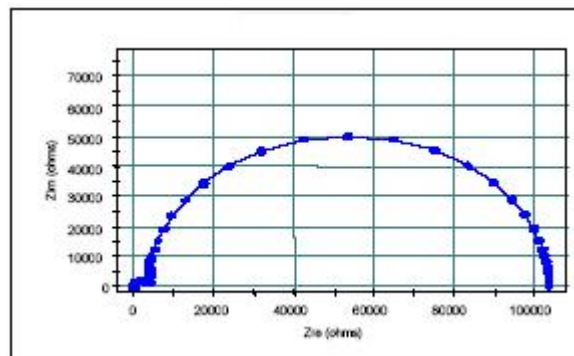


Figure 2-6. Nyquist Plot for a metal coated with a non-conductive film

Warburg Impedance

Diffusion of a reactant or a reaction product on the electrode surface can create impedance known as the Warburg Impedance. This situation can exist when the electrode is covered with adsorbed components, reaction products, or a prepared coating. This kind of behavior is shown in figure 2.7.

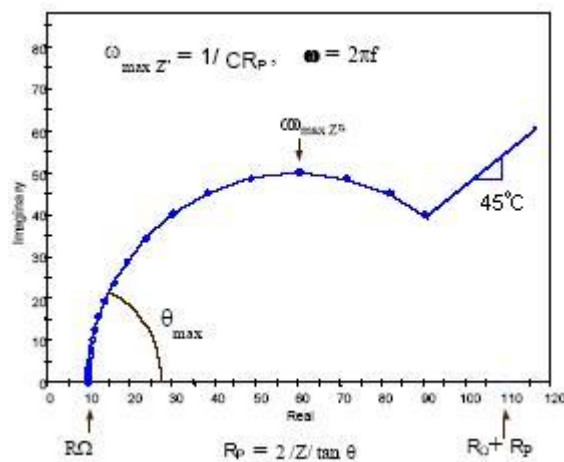


Figure 2-7. Nyquist Plot for Warburg Impedance behavior

The current is 45 degrees out of phase with the imposed potential; which means that the real and imaginary components of the impedance vector are equal at all frequencies. From the point of view of a simple equivalent circuit, the Warburg Impedance behavior is midway between a resistor (0 degree phase shift) and a capacitor (90 degree phase shift).

2.4.1.4.2 The Bode Plot

In this type of graph it is possible to understand how the impedance depends on the frequency. The impedance is plotted with log frequency on the X-axis and both the absolute value of the impedance ($|Z|$) and phase shift on the Y-axis. The plot in Figure

2.8 yields values of R_{Ω} reading directly $\text{Log}(R_{\Omega})$ from the high frequency horizontal level and, at lowest frequencies, polarization resistance, $\log(R_{\Omega} + R_p)$ reading from the low frequency horizontal level can be determined. . If a straight line with a slope equal to -1 is found at intermediate frequencies it is possible to find the value of C_D from the relationship:

$$|Z| = \frac{1}{C_D \omega}$$

where $\omega = 2\pi f$.

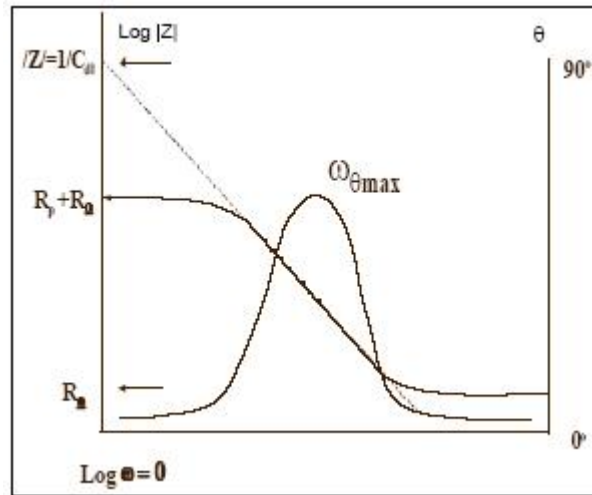


Figure 2-8. Bode Plot for a simple electrochemical system

$\text{Log } \omega$ and phase angle θ are also shown in the Bode Plot. At low and high frequency limits, where the behavior of the Randless Cell is a resistor, the phase angle is nearly zero, while at intermediate frequencies, θ increases as the imaginary component of the impedance increases. Thus, it is possible to determine the double layer capacitance (C_{DL})

where the phase shift of the response is maximum, and can be expressed with the following equation:

$$\omega_{(\theta=\max)} = \sqrt{(1/C_D R_p)(1 + R_p / R_\Omega)}$$

The Bode Plot is a useful alternative to the Nyquist Plot because it can avoid possible errors in the fitting of the Nyquist semicircle and the longer measurement times associated with low frequency, R_p , determination.

2.4.2 Potentiodynamic anodic polarization

Potentiodynamic anodic polarization is a direct current technique in which current and potential are the two fundamental variables. This evaluation method is used to determine the active-passive characteristics of a given metal-solution system.

This method involves a scan of the working electrode potential typically starting at -250 mV with respect to E_{corr} (the open circuit potential) and scanning in a positive direction, usually to a potential positive enough to oxidize the test solution. Generally a scan rate from 0.1 mV to 5 mV/s is used and the resulting curve is a plot of the potential versus the logarithm of the measurement current. A potentiodynamic curve is an indication of the corrosion behavior of the specimen and consists principally of a cathodic and anodic region, a passive region and a transpassive region. (Figure 2.9). From this curve it is possible to determine the anodic and cathodic Tafel slopes (β_a and β_c), the corrosion

current (I_{corr}), corrosion potential (E_{corr}), the passive and transpassive potential, and current. E_{corr} and I_{corr} are calculated by intersection of both anodic and cathodic Tafel slopes, while the other values are obtained directly from the curve.

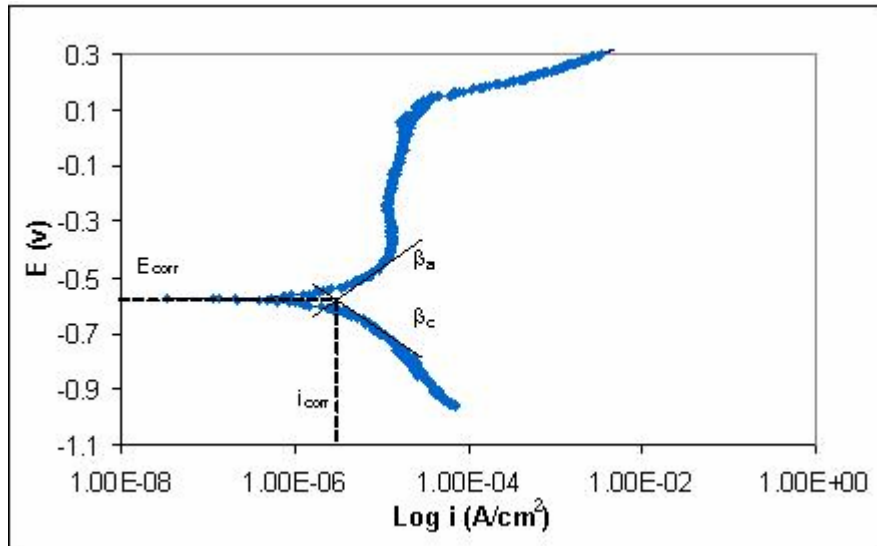


Figure 2-9. Potentiodynamic polarization curve

Corrosion current density is one of the most important parameters since it is directly related with corrosion rate (C_R). Once I_{corr} is determined the corrosion rate (in mm-in/year) can be calculated from the following equation:

$$C_R = \frac{i_{corr} A_w}{zF\rho}$$

Where: A_w = atomic weight (g/mol)

z = valence

F = Faraday's constant = 96500 (As/mol)

ρ = density

Potentiodynamic anodic polarization complies with some ASTM norms, which are listed below in Table 2.10.

Table 2-10. ASTM norms used for corrosion testing

ASTM Norm	DESCRIPTION
G 1-90	Practice for Preparing, Cleaning, and Evaluating Corrosion Test Specimens
G 3 - 89	Practice for Conventions applicable to Electrochemical Measurements in Corrosion Testing
G 5 - 94	Reference Test Method for Making Potentiostatic and Potentiodynamic Anodic Polarization Measurements
G 15 - 97a	Terminology Relating to Corrosion and Corrosion Testing
G 59 - 97	Practice for Conducting Potentiodynamic Polarization Resistance Measurements
G 102 - 89	Practice for Calculation of Corrosion Rates and Related Information from Electrochemical Measurements.

2.5 RECENT LITERATURE

For many years, titanium alloys have been considered as biomaterials due to their excellent compatibility, mechanical properties, and corrosion resistance. Hence, many studies have been carried out to evaluate their performance.

As mentioned earlier, corrosion resistance is an essential characteristic for a metallic biomaterial. Titanium alloys have excellent corrosion resistance because an

external oxide layer that forms when the material is in contact with the service medium protects these materials. Solar et al [11], characterized the passive film formed on Ti-6Al-4V surfaces in Ringer's solution where passivity was observed over the potential range of -400mV to +1400 mV versus saturated calomel electrode (SCE) without breakdown. Due to the existence of the passive layer, analytical techniques in combination with electrochemical oxidation have been explored to study quasi-in-situ, the formation of the oxide layer on Ti alloys. In a study by Milosev et al [12] of the passive film formed on TiAlV alloy with X-ray photoelectron spectroscopy and Electrochemical Impedance Spectroscopy (EIS), it was determined that the oxide layer was predominately titanium (IV) oxide. The metal oxide interface was enriched with titanium sub-oxides TiO and Ti₂O₃. The thickness of the layer formed by electrochemical oxidation, in this case in Hank's physiological solution, is dependent on the oxidation potential. In another study, Alexia et al [13] evaluated, by EIS and photoelectrochemistry, the evolution of the passive film formed on Ti, Ti-6Al-4V and Ti-6Al-7Nb when it is exposed to an electrolyte solution that contains Ca⁺² and PO₄³⁻. The results showed that calcium and phosphate ions selectively interact with the titanium dioxide passive film increasing its corrosion resistance.

Since the titanium oxide layer is porous and not tough [14] it is possible for the passive layer to be removed allowing active corrosion if the biomaterial is subjected to wear. For this reason the effect of wear on accelerating the corrosion of three titanium alloys, Ti-6Al-4V, Ti-6Al-7Nb, and Ti-13Nb-13Zr was studied by Khan et al [15] using cyclic polarization techniques under four different conditions: corrosion without wear,

wear-accelerated corrosion (part of the surface of each specimen was continuously abraded), wear in a corrosive environment (the samples were damaged continuously for a period of 10 min in phosphate buffered saline-PBS), and wear in a non-corrosive environment (the samples were damaged in distilled water for the same time period). In general, the results showed that degradation was lowest for Ti-13Nb-13Zr and highest for Ti-6Al-4V and Ti-6Al-7Nb.

So far, only studies of structural and mechanical characterization of thermal oxidation has been made on gamma titanium aluminide. There is no direct study about corrosion resistance of this titanium alloy at low temperatures, which is the scope of this research. Xia et al. [16] evaluated the microstructure, composition, and mechanical properties of the titanium oxide treated at 850°C for 8, 20, 50, and 100 hours with different techniques, such as X-ray diffraction, glow discharge spectroscopy, scanning electron microscope, and transmission electron microscopy. The results showed that the surface treatments created a stable and resistant multi-layered oxide scale consisting of rutile (TiO₂), and a mixture of Al₂O₃, Ti₂AlN, and TiN on γ -TiAl surface.

Only a few articles on the corrosion behavior of Ti-6Al-4V implant alloy in human body can be found in literature. In one, Wen-Wei et al. [17] studied the corrosion properties of this alloy in three biological solutions: urine, serum, and joint fluid using three different electrochemical techniques, such as, potentiodynamic polarization cyclic voltammetry and electrochemical impedance spectroscopy. It was found that the corrosion resistance for Ti-6Al-4V alloy in joint fluid was lower than in serum and urine.

Low values of I_{corr} and high values of E_{corr} obtained by Tafel analysis and higher values of R_p were found by electrochemical impedance spectroscopy in urine solution confirming that behavior. The experimental results obtained with AC and DC techniques were in good agreement with each other.

Unfortunately, the problem of corrosion is associated with the ion release of metallic materials, which can be harmful for the human body. It is for this reason that the alloys are surface treated to produce passive layers that increase the corrosion resistance. Many studies about this topic have been carried out, such as those performed by Marcianiak et al [18] where surface modifications such as grinding, electropolishing, and electrochemical passivation were done to Ti-6Al-4V. Subsequently these specimens were evaluated in Tyrone's solution by potentiodynamic tests. In another study carried out by Mizutani et al. [19] Ti-6Al-4V alloy's surface was modified by ELID (Electrolytic in-process Dressing), and electrochemical corrosion tests were carried out to evaluate its corrosion behavior. The processed surfaces were analyzed by means of X-ray photoelectron and Nano Hardness tester. The results showed higher corrosion resistance and hardness compared to the surface finished by polishing. In a study by Zhuo et al [20], different titanium alloys, such as CP titanium, Ti-6Al-4V, Ti6Al-7Nb, and Ti13Nb-13Zr were surface-modified by sandblasting and polishing treatments. The results obtained by linear polarization technique for all metals examined with the same surface conditions showed a similar behavior; but it was found that for Ti6Al-7Nb there were higher values of R_p (polarization resistance), and lower values of I_{corr} (corrosion rate), than for other alloys. X-ray photoelectron spectroscopy method detected hydrated Ti (IV) oxide, mainly

TiO₂ (rutile) with tetragonal structure on these metals surfaces, and Nb (V) oxide was identified on the Ti-6Al-7Nb surfaces. In another study, Gurappa [21] evaluated the corrosion characteristics of titanium alloy Ti-5.8Al-4.06Sn-3.61Zr-0.7Nb-0.54Mo which forms a passive layer at high temperatures. It was observed that the formation of a continuous and protective layer of alumina on its surface is necessary to use this alloy in applications with aggressive medium service.

Many studies [9,22] have been carried out on the effect of surface treatments. In the present research, titanium alloys were exposed at two different temperatures, 500°C and 800 °C, to force oxidation and increase their corrosion resistance. A similar study was carried by García-Alonso et al [9], where an evaluation of the influence of thermal oxidation of Ti-6Al-4V was done, but at 500°C and 700 °C for 1 hour on in-vitro corrosion behavior and osteoblast response. The anodic polarization curve indicated a high corrosion resistance for the surface treatment when it was exposed to Ringer's solution. In the evaluation made by Guleryuz et al [22] where Ti-6Al-4V was thermally oxidized, at 600°C and 650°C for 60 hours, its corrosion resistance increased with the formation of oxides layer composed of anatase and rutile structures of TiO₂.

Furthermore, titanium alloys with Ni as a component were evaluated with surface modifications. In a study carried out by Thierry [23] NiTi alloys were surface modified with different sterilization techniques such as dry heat, steam autoclaving, ethylene oxide, and peracetic acid. Then, analyses were performed by Auger electron spectroscopy, atomic force microscopy, and contact angle measurement, which proved the formation of

an oxide layer on the alloy surface. These alloys were also evaluated by Starosvetsky et al [24] who modified its surface properties using an original powder immersion reaction assisted coating known as PIRAC, a method based on the annealing of samples in atmosphere of highly reactive nitrogen at 900°C and 1000°C. This coating method showed considerable improvements in the corrosion behavior of NiTi alloy in Ringer's solution in comparison with untreated samples.

Vanadium, which is one of the principal alloy components of Ti-6Al-4V, has been considered toxic [14,15], and the possibility of ion release of this metallic species in the body made essential that many authors investigate this topic. Metikos et al [25] evaluated the influence of niobium and vanadium as alloying elements on titanium alloy passivity in Hank's balanced salt solution at 37°C. The titanium alloys studied were Ti-6Al-4V and Ti-6Al-6Nb by dc polarization and ac impedance spectroscopy techniques. The results showed a better behavior for Ti-6Al-6Nb than Ti-6Al-4V, attributed to the stabilizing effect of Nb⁵⁺ cations on the passive film. For Ti-6Al-4V, vanadium ion release produced a diffusion of vacancies in the oxide layer. This, coupled with the presence of chloride ions at high concentrations in the solution causes their absorption into oxygen vacancies on the surface. The stability of the oxide layer decreases and there is a possibility of a breakdown and pitting corrosion. This process ultimately causes corrosion susceptibility. Due to potential adverse effects of vanadium, a number of different Ti-based alloys without vanadium have been investigated. Lopez et al [14] studied the corrosion behavior of three non-vanadium containing titanium alloys; namely Ti-7Nb-6Al, Ti-13Nb-13Zr, and Ti-15Zr-4Nb by means of potentiodynamic polarization

and electrochemical impedance spectroscopy. The corrosion rates of these titanium alloys were very low compared with Ti-6Al-4V, which is the conventional biomaterial. The corrosion current densities (I_{corr}) were very stable with time, indicating a passive state. In general, the alloys containing Zr showed the best behavior, indicating a low susceptibility to localized corrosion in these alloys.

Previous studies have investigated the effect of different electrolytes on the repassivation of the alloys. In recent work carried out by Khan et al [15] the ability of Ti-6Al-4V, Ti-6Al-7Nb, and Ti-13Nb-13Zr to repassivate in environments in the presence of proteins was studied. This study showed that, in different environments, the ability of the alloys to repassivate is affected by the proteins, because it was found that corrosion reduced hardness of the surface oxides. In another study by Yong-Jae et al [26], three different alloys, $\text{Al}_{67}\text{Ti}_{25}\text{Cr}_8$, $\text{Al}_{66}\text{Ti}_{24}\text{Cr}_{10}$ and $\text{Al}_{59}\text{Ti}_{26}\text{Cr}_{15}$ were studied in 3.5 wt% NaCl solution. Electrochemical impedance spectroscopy and cyclic potentiodynamic polarization techniques showed that with higher chromium contents, E_{pit} and E_{prot} , pitting potential, and propagation potential, respectively, increased, thus, improving relative resistance to pit initiation and propagation.

There are many electrochemical techniques used to evaluate the corrosion behavior of biomaterials. In the present study anodic polarization technique and electrochemical impedance spectroscopy (EIS) will be used to evaluate γ -TiAl and Ti-6Al-4V. Many authors have used these methods to evaluate different materials. Ionipa et al. [27] evaluated Ti, Ti-5Al-4V, and Ti-6Al-4Fe with EIS to study the spontaneous passivation

of these alloys in Ringer's solution at different pH. Impedance spectra, in Nyquist and Bode plots were obtained at open circuit potential and at different potentials from the passive potential range. The results showed high values of resistance of the passive film for the three alloys ($R_p \sim 2 \text{ M}\Omega \cdot \text{cm}^2$), and a relatively low passive film capacitance value ($C_p \sim 15 \mu\text{F}/\text{cm}^2$), which decreased slightly with the potential. This behavior corresponds to a slow growth of the titanium oxide film indicating a long-term stability of the passive layer, which implies a good corrosion resistance.

This technique also was used to characterize the in situ growing process of osteoblast-like U-2 OS cells on polished Ti and Ti-6Al-4V alloy. This study was made by Hsiung [28] during 72 hours incubation to demonstrate that the biocompatibility of metal implants is related to their surface electrochemical characterization. The results showed that the presence of cells on metals led to increase in the impedance and polarization resistance (R_p) values. SEM micrographs and an equivalent circuit confirmed this behavior.

In addition, others authors such as Zeng et al [29], in two different studies, employed EIS in studying reaction mechanisms and kinetics of corrosion process. The first study consisted in evaluating the corrosion of B-1900 (Ni-Co-Cr-Mo-Al-Ti-Ta-C-Zr) alloy at 800°C in air, and in the presence of Na_2SO_4 and 25wt% NaCl-75wt% Na_2SO_4 . The impedance spectrums for the metal in both mediums were similar in that they were composed of a single capacitive loop, which can be represented by a parallel circuit with charge transfer resistance. The R_p values were higher for the alloy in Na_2SO_4 than in the

presence of NaCl- Na₂SO₄ by 50%. In the second study, the corrosion of the two-phase Ni-10Ti and Ni-15Ti in molten (0.62Li, 0.38K)₂CO₃ at 650°C in air was investigated. The impedance spectra were composed of a small semi-circle at high frequency and a line at low frequency, which is typical of a Warburg process. An equivalent circuit was made to describe this behavior and the R_p values found were relatively low for both mediums.

More recently, researchers have tried to control the corrosion problem on titanium alloys used as biomaterials. However, these alloys are not totally resistant to corrosion as in the case of Ti-6Al-4V. Thus, the purpose of this research is to study the corrosion resistance of the metallic alloy, γ -TiAl, to determine its feasibility as a metallic biomaterial alternative.

It is clear that Ti-based alloys have superior corrosion resistance and consequently γ -TiAl is expected to show similar behavior. Even though the corrosion behavior in Ringer's solution, 3.5% NaCl, and seawater of γ -TiAl has not been reported in open literature, the studies mentioned above provide experimental guidelines to be carried out in the present work to evaluate the performance of γ -TiAl, such as, the selection of potentiodynamic anodic polarization (PAP) and electrochemical impedance spectroscopy (EIS) as the appropriate techniques for corrosion evaluation of titanium alloys and surface modification of alloys at high temperatures as an alternative to improve its corrosion resistance.

3.1 Materials

The bulk composition of γ -TiAl alloy, commercially named Ti-48-2-2, is mainly 48 at% of Ti, 48 at% of Al, 2 at% of Cr, and 2 at% of Nb. This alloy in the form of 1 inch diameter rods in the as-received condition was produced from hot isostatically pressed powder. Commercial Ti-6Al-4V alloy also obtained as 1 inch rods in the annealed condition was used in this study for comparison. The approximate bulk composition of Ti-6Al-4V is 87.73 wt% of Ti, 6.85 wt% of Al and 5.42 wt% of V; complying with ASTM F 136 norm.

3.2 Sample preparation

Disc-shaped specimens with approximate thickness of 5/64 in. and a diameter of 5/8 in were machined from γ -TiAl and Ti-6Al-4V was using electric-arc discharge machine (EDM). Prior to testing, each specimen was mechanically ground with 240 grit followed by 600 grit paper in a Buehler Ecomet 3 for ten minutes with an applied force of 8 lb at 300 rpm for each paper. Finally, specimens were cleaned in an ultrasonic cleaner for five minutes with alcohol, followed by a rinse in distilled water. Figures 3.2 and 3.3 show the equipment used for the grinding and cleaning processes respectively.



Figure 3-2. Mechanical grinding process



Figure 3-3. Ultrasonic cleaning process

3.3 Pre-treatment

In order to evaluate the resistance of γ -TiAl and Ti-6Al-4V to corrosion for various surface modifications, each alloy was pre-treated by three different methods. These consist of i) a heat treatment to oxidize the samples at 500°C and ii) 800°C for one hour in air for both titanium alloys in a rapid heating furnace and iii) autoclaving process at 15 psi and 121°C for one hour for each alloy, respectively. Figure 3.4 shows the equipment used for the autoclaving process.



Figure 3-4. Autoclaving process

3.4 Sampling

Table 3.1 shows the experimental samples matrix that was used to carry out this research. In total, 192 samples were evaluated. 48 samples were studied each for γ -TiAl and Ti-6Al-4V respectively for each electrochemical technique, of which, twelve were oxidized at 500°C, twelve were oxidized at 800°C, twelve were subjected to autoclaving, and twelve were control samples. These control samples did not have any surface

treatment and their function was to establish the baseline behavior of titanium alloys to corrosion testing. Additionally, 96 more samples of control and autoclaving treatment were used to evaluate the temperature effects on the samples at 25°C, 30°C, and 37°C, respectively.

The corrosion behavior of the Ti alloys was evaluated at room temperature using three different electrolytes: i) Ringer's solution, which simulates the body fluids with $\text{pH} \bar{6}$, viscosity of 0.676 cP, and a chemical composition for each 100 ml, of 600 mg of sodium chloride, 310 mg of sodium lactate, 30 mg potassium chloride, and 20 mg of calcium chloride, ii) seawater compose of 20567.2 ppm of chlorides, 2750.3 ppm of sulfates, calcium, magnesium, with a viscosity of 0.95 cP, and $\text{pH} \bar{6}$ and iii) 3.5 wt% NaCl with $\text{pH} \bar{6}$, the most common electrolyte used for corrosion testing and evaluation with a viscosity of 0.913 cP. The volume of the electrolyte used for each test was 600 ml, and the pH values of the three electrolytes were measured before testing. For each experimental condition, four (4) samples were tested to obtain an acceptable average from these results.

3.5 Sample characterization

With the purpose of characterizing the samples and determining if the pre-treatments were effective, two material characterization methods were employed: scanning electron microscopy (SEM) and X-ray diffraction patterns (XRD). The SEM was a JEOL-JSM-5410 and the XRD machine was a SIEMENS D5000 Diffractometer.

The SEM operational parameters were those commonly used for a metallic material evaluation, which are, spot size 8, aperture 60 μm , bias 50, and 15 kV for magnifications between 200X to 10000X. The parameters used for XRD to identify the passive layer were a range between 20.00° and 80.00° for 2θ angle and a step time of 1 s. The samples of γ -TiAl and Ti-6Al-4V with oxidation treatment at 500°C and 800°C , control and autoclaving samples, were transversally cut and examined with SEM to determine the presence of an oxide layer. The XRD method was used to characterize the autoclaved samples at different times: 15 min, 1hr, 2 hr, and 3 hr to determine if the stable oxide layer grew as the exposure time for this process increased. Optical microscopy and backscatter methods were used to observe the microstructure of titanium alloys. Metallographic preparation included mounting the samples in a cold curing resin and polishing with Mastermet 2R to maintain the oxide layer intact.

3.6 Evaluation by electrochemical methods

The experimental setup for the electrochemical measurement consisted of a three-electrode glass cell (K-cell). A standard calomel electrode (SCE) was used as the reference electrode which makes contact with the solution through a bridge tube, and the counter electrode consisted of two graphite rods positioned symmetrically relative to the working electrode (test specimen), supplying the current. The exposed surface area of γ -TiAl and Ti-6Al-4V was 1.0 cm^2 . Figure 3.5 shows the K-cell used for the electrochemical corrosion measurement.

Table 3-1. Experimental matrix

MATERIAL: GAMMA TITANIUM ALUMINIDE						MATERIAL: Ti-6Al-4V					
TYPE	ELECTROLYTE	M-1	M-2	M-3	M-4	TYPE	ELECTROLYTE	M-1	M-2	M-3	M-4
Control	3.5% NaCl	√	√	√	√	Control	3.5% NaCl	√	√	√	√
	Ringer's Solution	√	√	√	√		Ringer's Solution	√	√	√	√
	Seawater	√	√	√	√		Seawater	√	√	√	√
Oxidation 500 C	3.5% NaCl	√	√	√	√	Oxidation 500 C	3.5% NaCl	√	√	√	√
	Ringer's Solution	√	√	√	√		Ringer's Solution	√	√	√	√
	Seawater	√	√	√	√		Seawater	√	√	√	√
Oxidation 800 C	3.5% NaCl	√	√	√	√	Oxidation 800 C	3.5% NaCl	√	√	√	√
	Ringer's Solution	√	√	√	√		Ringer's Solution	√	√	√	√
	Seawater	√	√	√	√		Seawater	√	√	√	√
Autoclaving	3.5% NaCl	√	√	√	√	Autoclaving	3.5% NaCl	√	√	√	√
	Ringer's Solution	√	√	√	√		Ringer's Solution	√	√	√	√
	Seawater	*	*	*	*		Seawater	*	*	*	*
CONTROL						CONTROL					
Temperature Effect		M-1	M-2	M-3	M-4	Temperature Effect		M-1	M-2	M-3	M-4
25 C	Ringer's Solution	√	√	√	√	25 C	Ringer's Solution	√	√	√	√
30 C	Ringer's Solution	√	√	√	√	30 C	Ringer's Solution	√	√	√	√
37 C	Ringer's Solution	√	√	√	√	37 C	Ringer's Solution	√	√	√	√
AUTOCLAVING						AUTOCLAVING					
Temperature Effect		M-1	M-2	M-3	M-4	Temperature Effect		M-1	M-2	M-3	M-4
25 C	Ringer's Solution	√	√	√	√	25 C	Ringer's Solution	√	√	√	√
30 C	Ringer's Solution	√	√	√	√	30 C	Ringer's Solution	√	√	√	√
37 C	Ringer's Solution	√	√	√	√	37 C	Ringer's Solution	√	√	√	√

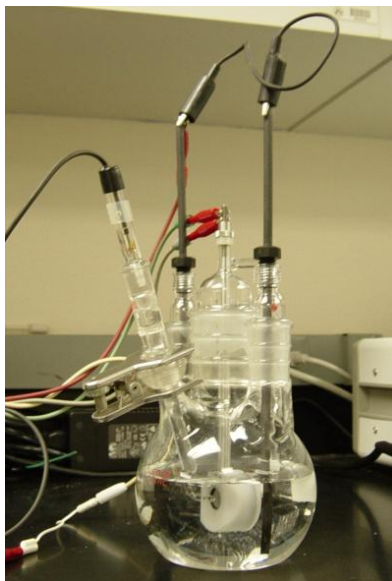


Figure 3-5. Electrochemical cell (K-cell)

A commercially available computer package was used to process data acquisition. Princeton Applied Research developed this multi-package, called PowerSuite, and contains PowerSine and PowerCorr, the two programs used in this research to evaluate the corrosion behavior of titanium alloys at alternate current and direct current respectively. PowerCorr was used to make the measurements for the polarization curves. The anodic polarization curves were recorded at a potential scan from -1.0 V to 0.800 V versus open circuit potential and a scan rate of 20 mV/s. Quantitative analyses from the polarization curves were made to determine E_{corr} (corrosion potential), I_{corr} (corrosion current), and cathodic and anodic Tafel slopes. The corrosion rate, C_R (rate of metal dissolution), in millimeters per year was determined with a standard equation [30].

PowerSine was used to evaluate the samples with electrochemical impedance spectroscopy technique. This method is conducted according to the ASTM G-106 standard practice. The AC impedance spectra for γ -TiAl and Ti-6Al-4V alloys were obtained at the open circuit potential, with a scan frequency range of 100 kHz to 1 mHz with amplitude of 10 mV for 36 experimental points. Nyquist plots and Bode plots were obtained and analyzed to determine the solution resistance (R_{Ω}), polarization resistance at the electrode/solution interface (R_p), and a double layer capacitor at this interface (C_{DL}). Each EIS test had a duration of, approximately, one hour.

The corrosion measurements for each experimental condition were carried out using a potentiostat/galvanostat (Parstat 2263, EG & G Princeton Applied Research). Figure 3.5 shows the experimental setup used for the electrochemical corrosion measurement. To evaluate the temperature effect on the samples, a Precision 180 Series Water Bath was used to maintain the desired temperature for electrochemical measurements. Figure 3.6 shows the experimental setup used for this purpose.



Figure 3-6. Experimental setup for corrosion measurements

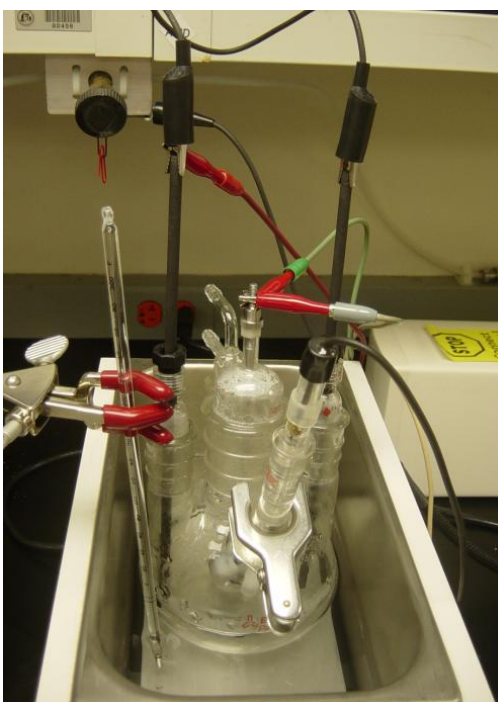


Figure 3-7. Experimental setup for evaluation at different temperatures

4 RESULTS AND DISCUSSION

Determining the corrosion behavior of a material as an integral part of its biocompatibility is critical in its approval as a biomaterial. In this research, γ -TiAl was evaluated with two electrochemical techniques in three different electrolytes to determine its performance. Ti-6Al-4V was used as the biomaterial for comparison. For this purpose, preliminary characterization of these materials with special techniques such as SEM and XRD were performed to aid in the analysis of experimental results.

4.1 Characterization

4.1.1 Materials

Micrographs of γ -TiAl and Ti-6Al-4V were obtained with optical microscope and electron backscattering using the SEM. Figure 4.1 shows the optical microstructure and the backscattered electron image for γ -TiAl. This alloy mainly consists of 80 vol. % lamella with $\sim 300\mu\text{m}$ colony size and 20 vol. % blocky gamma grains. Figure 4.2 shows the microstructure of Ti-6Al-4V obtained with optical microscope and backscattered SEM. In the as-received condition, this alloy clearly shows a duplex ($\alpha+\beta$) microstructure containing small equiaxed grains of α (light) with intergranular beta (dark).

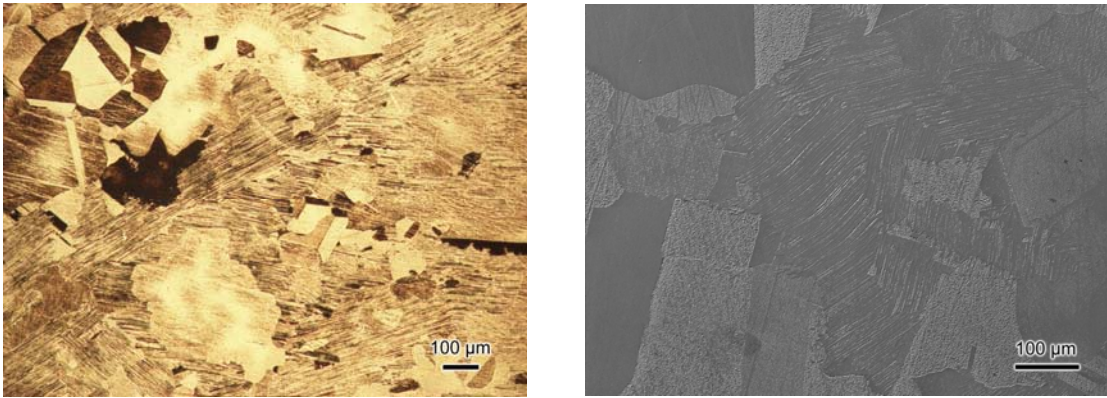


Figure 4-1. Microstructure of γ -TiAl (a) optical image (b) backscattered electron image

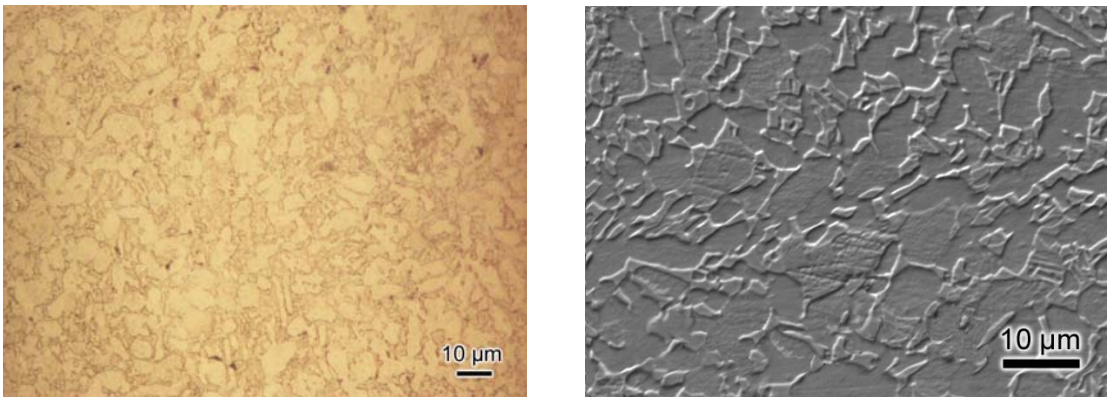


Figure 4-2. Microstructure of Ti-6Al-4V (a) optical image (b) backscattered electron image

XRD patterns confirmed that the as-received Ti-48Al-2Nb-2Cr reveals the presence of titanium aluminum with a tetragonal structure as shown in Figure 4.3. The XRD pattern for Ti-6Al-4V is shown in Figure 4.4.

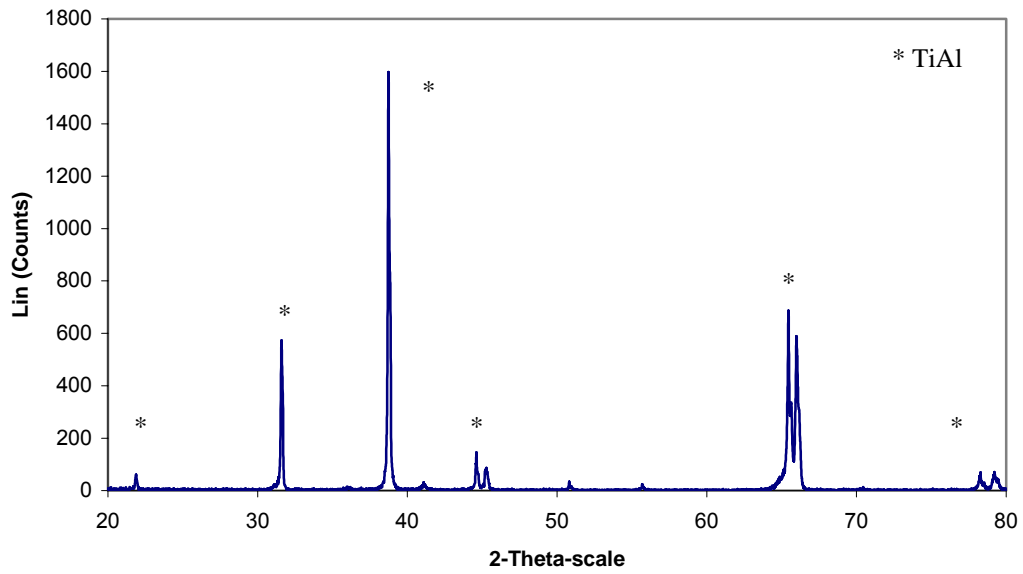


Figure 4-3. XRD pattern of as-received (control) sample of γ -TiAl

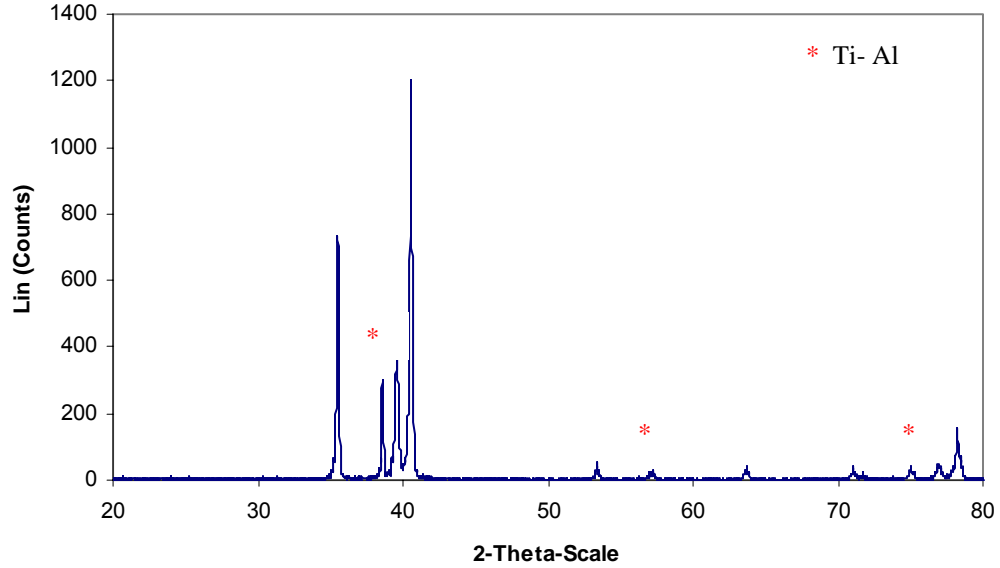


Figure 4-4. XRD pattern of as-received (control) sample of Ti-6Al-4V

4.1.2 Pre-treatments

For the purpose of identifying the presence of a passive layer on titanium alloys, SEM micrographs of the sample cross-section were taken. SEM micrographs of the cross-section of the control samples were observed for comparison. XRD was the characterization method used to determine possible composition of the passive layer.

4.1.2.1 γ -TiAl

Figure 4.5 shows the comparison between the cross sectional images obtained with SEM for γ -TiAl: without treatment, after autoclaving for 1 h, and after oxidation treatment at 500°C and 800°C. The sample was observed using a scanning electron microscope (SEM) by mounting it in a polymeric resin. In the figure, the light side corresponds to metal (M), while the dark side is the polymeric resin (P). In this figure, the formation of an oxide layer on γ -TiAl can be identified for the different treatments. The oxide layer formed as a result of the autoclaving process has a size of 10 μ m, while the oxide layer size was determined to be 10 μ m and 1 μ m for oxidation at 500°C and 800°C, respectively.

XRD patterns of the treated samples are shown in Figure 4.6. Even though the SEM micrograph shows the clear presence of an oxide layer formed after autoclaving process, the XRD pattern does not show a significant difference in comparison with the control sample. This can be due to the very thin oxide layer formed. After thermal oxidation,

diffraction peaks of TiO_2 , a titanium oxide named Rutile, appeared and, increasing treatment temperature, the peak intensities of this oxide increased. In a study made by Xia et al [16] the same titanium alloy was thermally oxidized at 850°C in air for a long period. For 8 hrs they found diffraction peaks of TiO_2 and Al_2O_3 for 20 hr. Peaks of Ti_2AlN and TiN also appeared in addition to these oxides for increasing treatment time to 100 hr; the peaks intensities of both TiO_2 and Al_2O_3 increased. The results found in this study can point to the possibility of formation of new oxides with this type of treatment, such as, aluminum oxide that improve the corrosion resistance of this alloy if the time increased.

As with most thermochemically treated materials, the oxidized scale consists of an oxide layer on the surface and a diffusion zone. In the same study Xia et al [16], used SEM to evaluate the oxide layer formed. They found the presence of several sub-layers designated as I, II, III, and IV. It was found that sub-layer I consisted of rutile- TiO_2 with equi-axed grains $0.4\text{-}1.0\ \mu\text{m}$ in size, sub-layer II consisted of $\alpha\text{-Al}_2\text{O}_3$ with traces of $\beta\text{-Al}_2\text{O}_3$, sub-layer III was a mixture of $\alpha\text{-Al}_2\text{O}_3$ and rutile- TiO_2 while Ti_2AlN and TiN with hexagonal structure were found in sub-layer IV.

The appearance of the $\gamma\text{-TiAl}$ surface after thermal oxidation varies from gray to yellow. This behavior is attributed to gradually increased saturation of oxygen in the alloy surface [16]. At 500°C the surface of $\gamma\text{-TiAl}$ was covered with a blue colored oxide layer attributed to the presence of Al_2O_3 , while at 800°C , the surface was covered with a dark yellow oxide due to presence of rutile- TiO_2 .

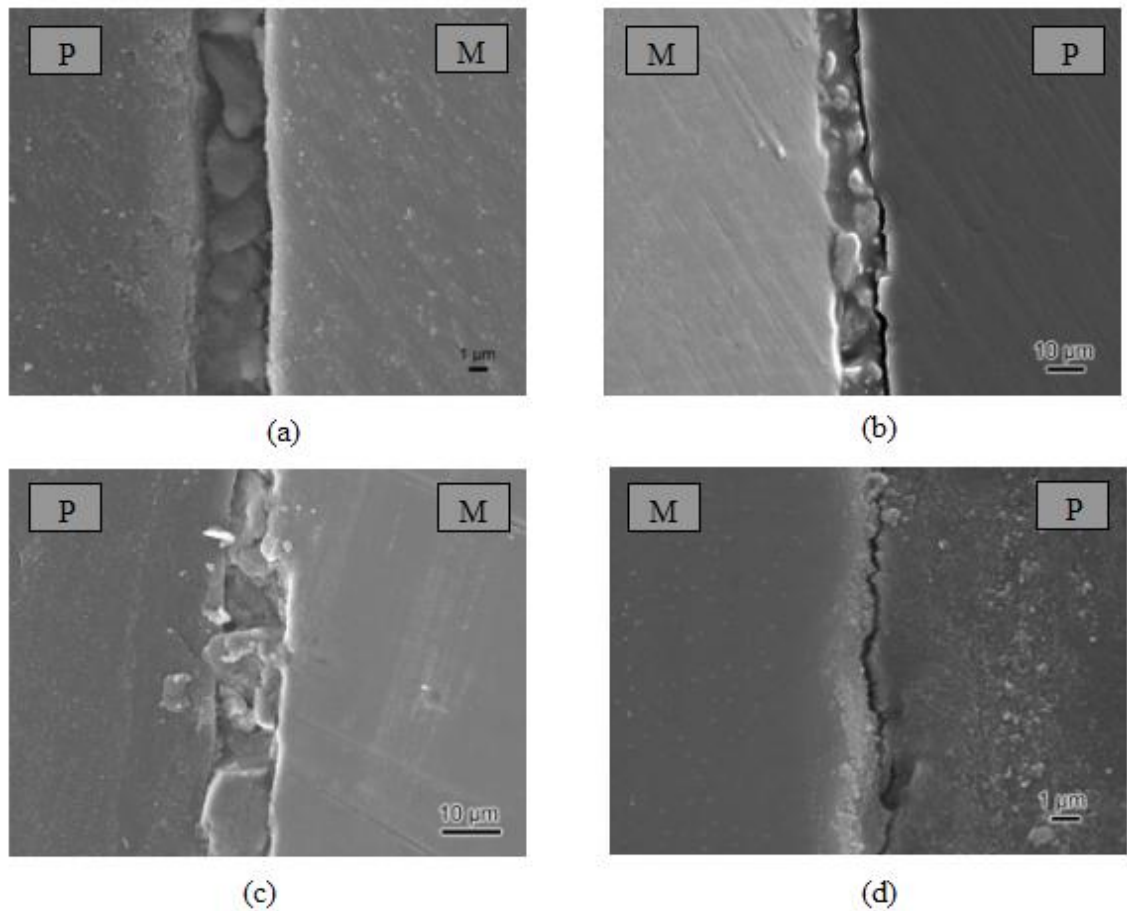


Figure 4-5. Cross sectional SEM micrographs of γ -TiAl (P: polymeric resin, M: metal)
 (a) control sample, (b) autoclaved sample, (c) oxidation treatment at 500°C,
 (d) oxidation treatment at 800°C

Earlier studies [16] have determined that the scale formed on γ -TiAl at high temperatures is commonly multilayered. It consists of a mixture of TiO_2 (rutile) in the outer layer, and a combination of TiO_2 and Al_2O_3 in the middle layer. TiO_2 is considered an oxygen-deficient oxide, can include titanium interstitials and oxygen vacancies, and generally is stable at 800°C. At 500°C a continuous layer of Al_2O_3 is preferentially formed. For Ti-6Al-4V at temperatures between 500°C and 800°C it is expected that stable layers of titanium oxides, namely rutile and anatase [9] be formed.

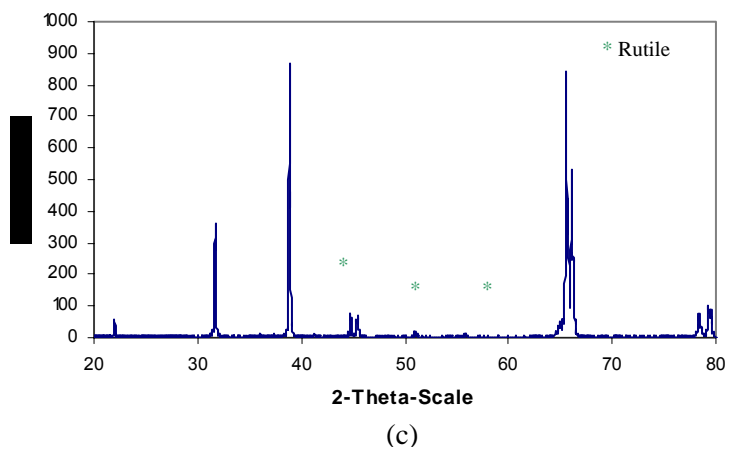
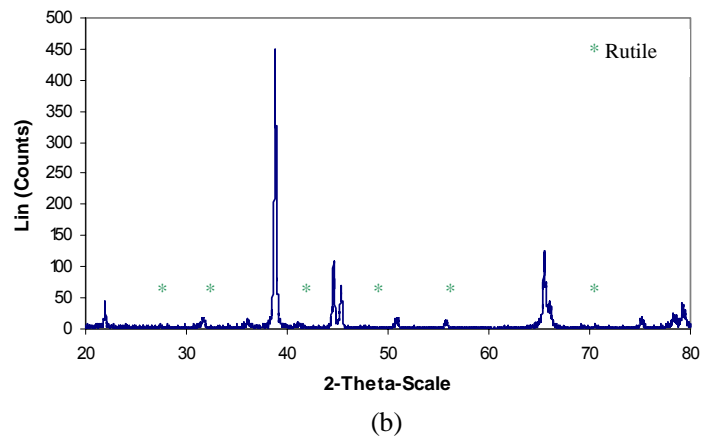
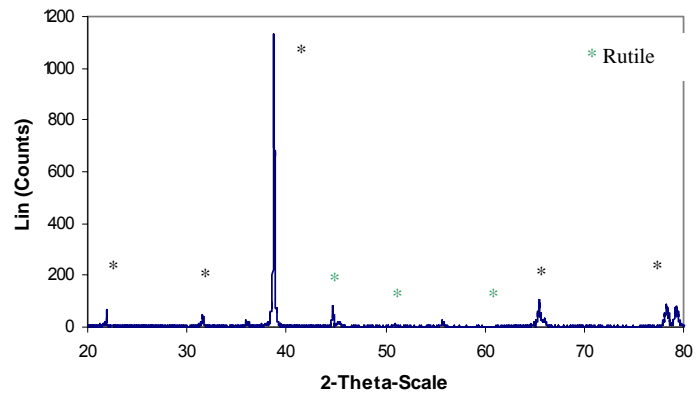


Figure 4-6. XRD pattern after treatment of γ -TiAl (a) autoclaved sample, (b) oxidation treatment at 500°C, (c) oxidation treatment at 800°C

4.1.2.2 Ti-6Al-4V

The same type of characterization was made for Ti-6Al-4V to determine the presence of an oxide layer formed with the treatments. Figure 4.7 show the cross-sectional view obtained with SEM for as-received (control) and autoclaved samples and samples oxidized at 500°C and 800°C. From these micrographs the formation of a thin layer between 1µm and 2µm is seen for autoclaved samples, and samples with oxidation at 500°C, respectively, while a thicker layer was observed for samples with treatment at 800°C with an approximate thickness of 10 µm.

To determine the possible composition of the oxide layers, XRD patterns were obtained from the samples. Figure 4.8 shows the comparison between the XRD patterns. Similar to the case of γ -TiAl, the XRD pattern for autoclaved samples of Ti-6Al-4V did not show any change, even though the SEM image shows the presence of a thin oxide layer. The formation of an oxide layer can be reflected in a shift of the peaks in the XRD patterns, but this behavior is not observed in this case. In contrast to the oxidized samples of γ -TiAl, the oxide layer size for Ti-6Al-4V increased with increasing oxidation temperatures from 2µm to 10µm for 500°C and 800°C, respectively. The results of XRD patterns for samples treated at 500°C revealed the presence of a titanium oxide Ti_6O with a hexagonal structure while the XRD patterns of the samples treated at 800°C indicated that the surface film contained mainly two titanium oxides TiO_2 , namely, rutile and anatase, both with a tetragonal structure.

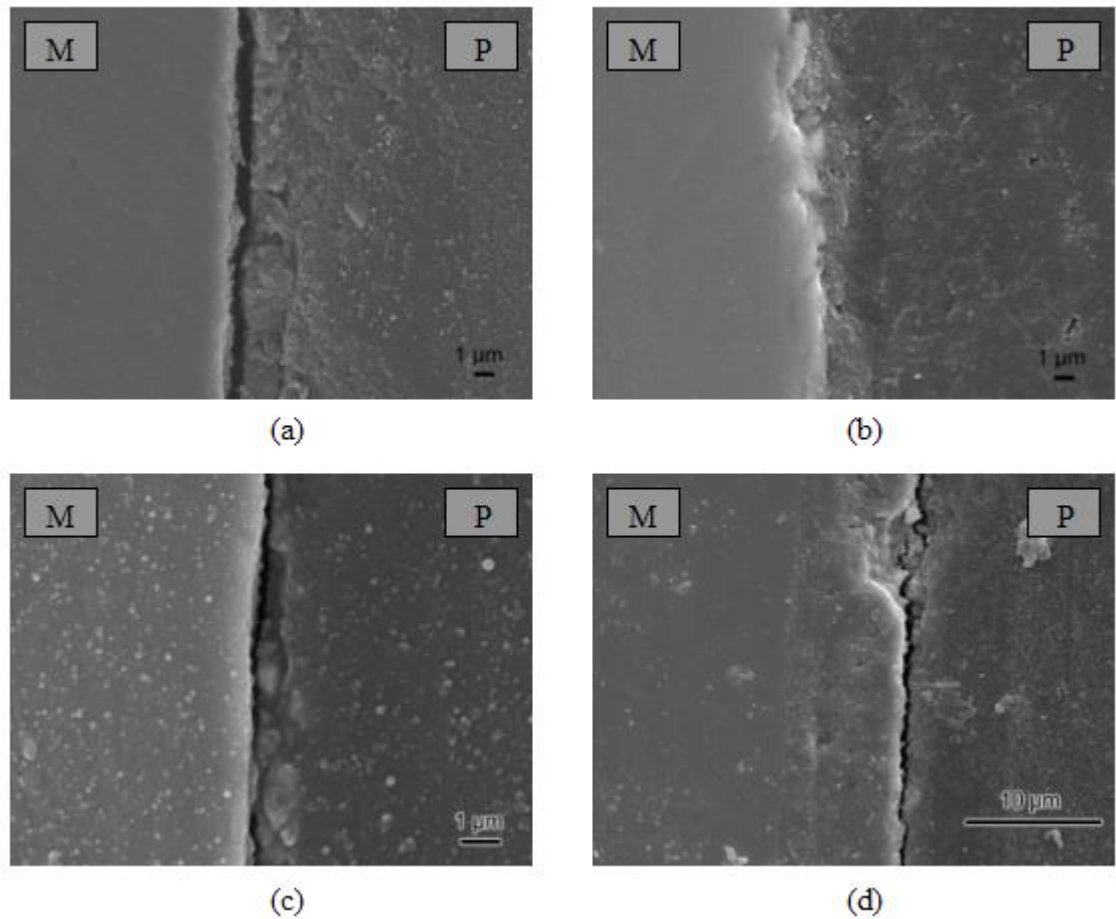
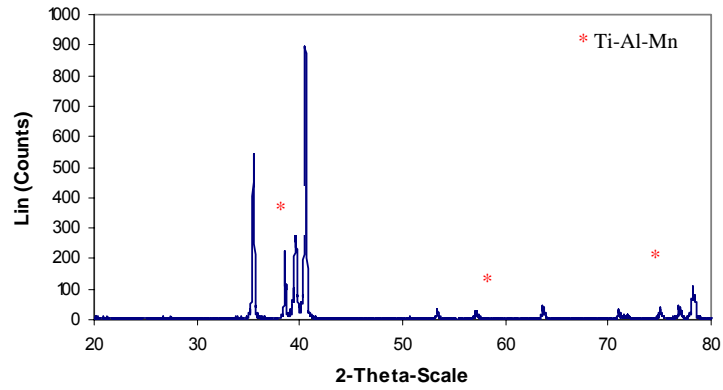


Figure 4-7. Cross sectional SEM micrographs of Ti-6Al-4V (P: polymeric resin, M:metal) (a)control sample, (b) autoclaved sample, (c) oxidation treatment at 500°C, (d) oxidation treatment at 800°C

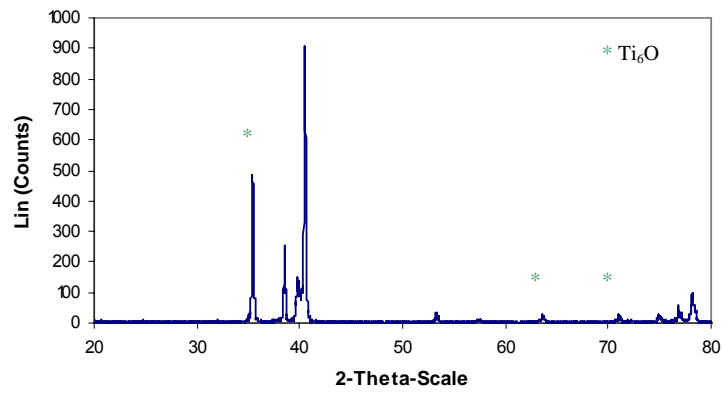
Some authors [13,31] have shown that exposure of the Ti-6Al-4V alloy to air spontaneously results in the formation of a passive oxide layer, which is predominantly TiO_2 and whose thickness varied from 2 nm to 7 nm. In the present research, the presence of an oxide layer of untreated sample was not identified from the XRD pattern, but a detailed observation of SEM micrograph revealed the presence of a thin layer, of approximately 0.1 μm . This layer was bigger than the one found in earlier studies [13,31] and is formed due to an extreme affinity of titanium to oxygen.

The presence of aluminum oxide is not detected by XRD patterns for the Ti-6Al-4V samples, in contrast to a study made by Hsiung [28] where X-ray photoelectron spectrometer (XPS) and Auger electron spectrometer (AES) indicated that the outermost surface film of Ti-6Al-4V alloy contained mainly TiO₂ and small amounts of Al₂O₃ and V₂O₅.

After thermal oxidation the surface of Ti-6Al-4V alloy was covered with a dark colored oxide layer similar to that obtained in a study made by Guleryuz et al. [22], where thermal oxidation treatment for Ti-6Al-4V at 600°C and 650°C between 12 to 60 hrs was made. XRD patterns of the untreated samples showed α -Ti and β -Ti peaks at different diffraction angles corresponding to different crystallographic planes, while, for oxidized surfaces, the results showed the presence mainly of rutile and anatase. The latter titanium oxide was only detected at limited number of diffraction angles, especially after oxidation at 600°C, while at 650°C rutile totally dominated the oxide structure. In the same study, cross-sectional optical micrographs of the oxidized samples were taken. As in the present study, an oxide layer and an oxygen diffusion zone appeared, and increasing oxidation temperature promoted the formation of a thicker oxide layer. The results from this study were further corroborated by comparison to a study made by Garcia-Alonso et al. [9], where Ti-6Al-4V was thermally oxidized at 500°C and 700°C. They evaluated, by means of a radio frequency glow discharge optical emission source (GDOES), the presence of oxidation products and found that rutile was the main oxide component produced with these treatments but did not discard the presence of other oxidation products.



(a)



(b)

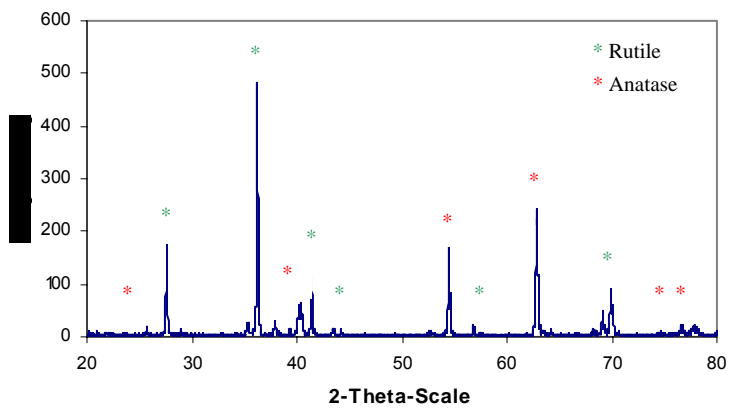


Figure 4-8. XRD pattern after treatment of Ti-6Al-4V (a) autoclaved sample, (b) oxidation treatment at 500°C, (c) oxidation treatment at 800°C

4.1.3 Characterization of autoclaved samples

The autoclaving process is one of the surface treatments least used on titanium alloys to improve corrosion resistance. However, a recent study, [7] showed the possibility that this type of treatment could increase biocompatibility of titanium alloys. Since the objective of this research is to study feasibility of γ -TiAl alloy as an alternative biomaterial, a fairly detailed study was carried out about the effect of autoclaving on γ -TiAl. For this purpose, γ -TiAl was exposed to 121°C and 15 psi autoclaving for different times: 15 min, 1 hr, 2 hr, and 3 hr to determine possible changes if any at all in its surface composition. For comparison, a parallel study was done on Ti-6Al-4V.

The X-ray diffraction (XRD) technique was used for this characterization; Figure 4.9 and Figure 4.10 show the comparison between the XRD patterns at different autoclaving times for γ -TiAl and Ti-6Al-4V. As was mentioned previously, this technique did not detect oxidation products obtained with the autoclaving treatment; but SEM imaging did showed the presence of these products. As can be seen in the diffractograms, a similar behavior for both alloys was obtained. No new surface products were detected with increasing autoclaving time.

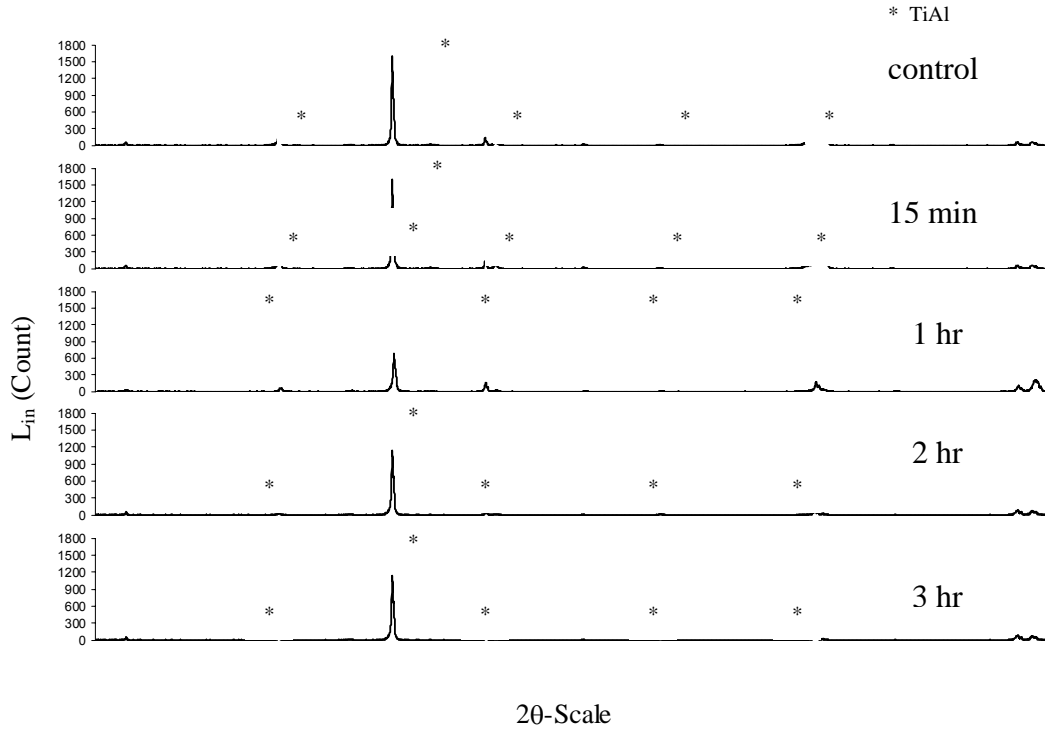


Figure 4-9. Comparison between XRD patterns of γ -TiAl for the different autoclaving times

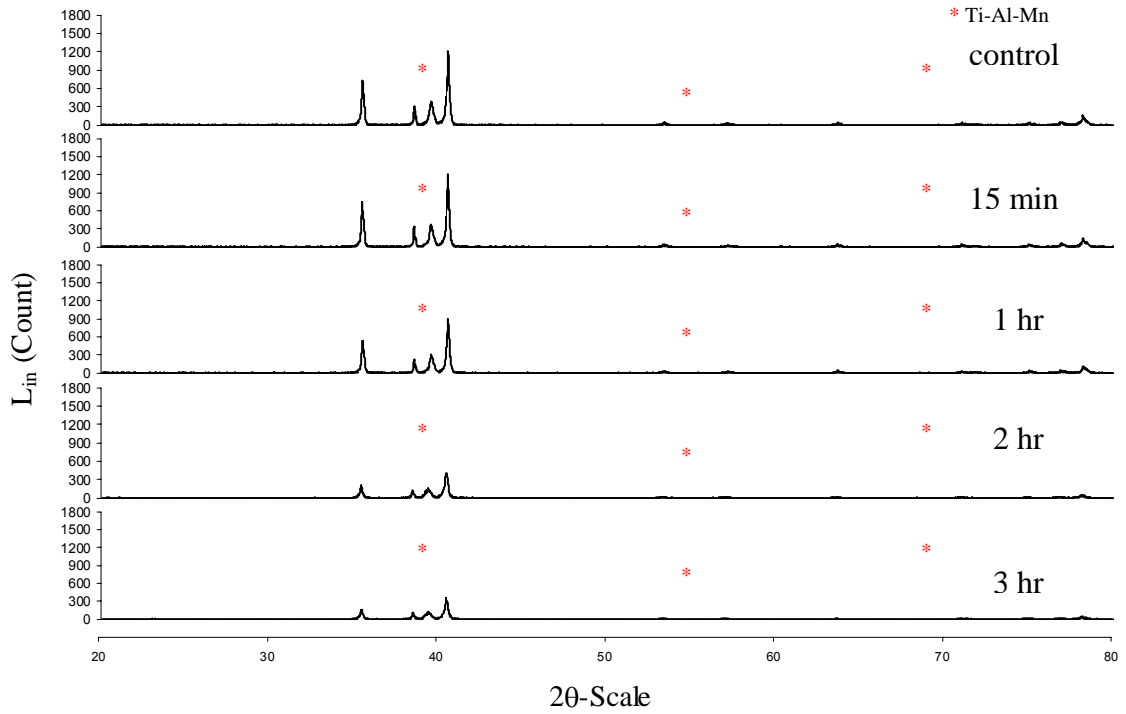


Figure 4-10. Comparison between XRD patterns of Ti-6Al-4V for the different autoclaving times

4.2 Evaluation by Electrochemical methods

Many studies have been carried out to electrochemically evaluate Ti-6Al-4V for corrosion resistance [9,13,15,17,33]; however, for γ -TiAl, a direct study on the corrosion resistance has not been reported in literature. In the present work, two electrochemical methods were chosen to evaluate the corrosion behavior of these alloys; namely potentiodynamic anodic polarization (PAP) and electrochemical impedance spectroscopy (EIS).

4.2.1 Potentiodynamic anodic polarization (PAP)

Potentiodynamic anodic polarization is a dc technique used to evaluate the corrosion behavior of γ -TiAl and Ti-6Al-4V. To infer a high corrosion resistance of titanium alloys experimentally using this method, high values of E_{corr} and low values of i_{corr} would be expected from polarization curves. Corrosion rate (C_R), the parameter that directly estimates corrosion resistance of materials, is determined from i_{corr} , and should have the lowest value possible.

Table 4.1 and Table 4.2 present the results obtained for γ -TiAl and Ti-6Al-4V. These tables show values of corrosion potential (E_{corr}), corrosion current densities (i_{corr}), anodic and cathodic Tafel slopes (β_a and β_c), and corrosion current (C_R). This last parameter was calculated with a standard equation.

As shown in Table 4.1, samples of γ -TiAl without superficial treatment were the only samples that showed a complete polarization curve that allows the determination of

corrosion parameters. Samples with surface treatments show a completely passive behavior.

Table 4-1. Corrosion parameters of γ -TiAl for all treatments

MATERIAL	TREATMENT	ELECTROLYTE	β_a	β_c	E _{corr}	i _{corr}	C _R
			(mV/decade)	(mV/decade)	(V)	($\mu\text{A}/\text{cm}^2$)	(mm/y)
γ -TiAl	Control	3.5 % NaCl	551.28 \pm 26.3	555.09 \pm 36.5	-0.615 \pm 0.056	1.94 \pm 0.38	1.80E-02 \pm 0.032
γ -TiAl	Control	Ringer's solution	556.51 \pm 38.2	373.78 \pm 21.9	-0.639 \pm 0.083	2.56 \pm 0.73	4.40E-02 \pm 0.021
γ -TiAl	Control	Seawater	499.9 \pm 51.4	612 \pm 49.7	-0.735 \pm 0.071	8.24 \pm 0.82	4.87E-02 \pm 0.057
γ -TiAl	Oxidation at 500C	3.5 % NaCl		PASSIVE			
γ -TiAl	Oxidation at 500C	Ringer's solution		PASSIVE			
γ -TiAl	Oxidation at 500C	Seawater		PASSIVE			
γ -TiAl	Oxidation at 800C	3.5 % NaCl		PASSIVE			
γ -TiAl	Oxidation at 800C	Ringer's solution		PASSIVE			
γ -TiAl	Oxidation at 800C	Seawater		PASSIVE			
γ -TiAl	Autoclaving	3.5 % NaCl		PASSIVE			
γ -TiAl	Autoclaving	Ringer's solution		PASSIVE			
γ -TiAl	Autoclaving	*		*			

Table 4-2. Corrosion parameters of Ti-6Al-4V for all treatments

MATERIAL	TREATMENT	ELECTROLYTE	β_a	β_c	E _{corr}	i _{corr}	C _R
			(mV/decade)	(mV/decade)	(V)	($\mu\text{A}/\text{cm}^2$)	(mm/y)
Ti-6Al-4V	Control	3.5 % NaCl	901.55 \pm 31.7	1069.33 \pm 48.9	-0.655 \pm 0.031	3.52 \pm 0.27	1.67E-02 \pm 0.027
Ti-6Al-4V	Control	Ringer's solution	356.89 \pm 28.9	270.04 \pm 32.3	-0.599 \pm 0.029	0.21 \pm 0.42	2.44E-03 \pm 0.042
Ti-6Al-4V	Control	Seawater	551.09 \pm 36.3	689.5 \pm 26.3	-0.635 \pm 0.036	1.6 \pm 0.25	5.48E-02 \pm 0.039
Ti-6Al-4V	Oxidation at 500C	3.5 % NaCl		PASSIVE			
Ti-6Al-4V	Oxidation at 500C	Ringer's solution	388.86 \pm 28.6	229.1 \pm 46.2	-0.174 \pm 0.027	0.75 \pm 0.17	7.45E-03 \pm 0.035
Ti-6Al-4V	Oxidation at 500C	Seawater		PASSIVE			
Ti-6Al-4V	Oxidation at 800C	3.5 % NaCl	463.7 \pm 47.2	414.98 \pm 30.3	-0.147 \pm 0.042	0.14 \pm 0.45	1.65E-03 \pm 0.046
Ti-6Al-4V	Oxidation at 800C	Ringer's solution	507.59 \pm 39.1	255.73 \pm 29.9	0.054 \pm 0.019	0.19 \pm 0.31	.23E-03 \pm 0.028
Ti-6Al-4V	Oxidation at 800C	Seawater	673.96 \pm 22.3	636.15 \pm 37.4	-0.108 \pm 0.035	0.22 \pm 0.27	2.59E-03 \pm 0.019
Ti-6Al-4V	Autoclaving	3.5 % NaCl		PASSIVE			
Ti-6Al-4V	Autoclaving	Ringer's solution		PASSIVE			
Ti-6Al-4V	Autoclaving	*		*			

The Tafel slope (β_a , β_c) values obtained for γ -TiAl control samples were high. This is a desired result since high values of Tafel slopes correspond to high values of corrosion potential and low values of corrosion current. Typical Tafel slopes in Fuel Cell systems are in the order of 30 to 120 mV/decade. Comparing the behavior for these samples in the three electrolytes, the samples evaluated in Ringer's solution showed the best

behavior due to low values of C_R . This is a positive result since among the three media used, Ringer's solution is the one that best simulates a human body fluid environment. Even for samples with no surface treatment, the results obtained would prove that the material has the excellent corrosion resistance required for biomaterial applications. Additionally, from Table 4.1, it is also important to note that the samples with surface treatments show a completely passive behavior as deduced from the polarization curve. This performance is expected due to the presence of a tough, continuous oxide layer formed with the surface treatments, producing additional protection on the samples. The presence of a passive layer on the alloy is characteristic of a passive zone in the polarization curve.

Values for the corrosion parameters, obtained for Ti-6Al-4V, are shown in Table 4.2. Similar results were obtained when comparing the corrosion parameters for control Ti-6Al-4V samples and the Ti-6Al-4V samples oxidized at 800°C in Ringer's solution. This alloy showed the best corrosion resistance under these conditions. Figure 4.11 shows the polarization curves obtained for samples oxidized at 800°C in the three electrolytes, where this behavior can be observed. Contrasting with γ -TiAl, the corrosion parameters for oxidation at 800°C of Ti-6Al-4V can be determined and low values of i_{corr} in the range of 0.14-0.21 $\mu\text{A}/\text{cm}^2$ and larger positive E_{corr} values were observed in comparison with the other treatments. This behavior represents an excellent corrosion resistance attributed to the presence of a passive layer of TiO_2 , rutile, on this alloy. For samples oxidized at 500°C, the corrosion parameters obtained for samples evaluated in

Ringer's solution, show low values of C_R . The results obtained for this treatment in the other electrolytes and for autoclaved samples indicate a complete passive behavior such as that found for γ -TiAl. Figure 4.12 shows the comparison between the anodic polarization curves for Ti-6Al-4V control in 3.5% NaCl, Ringer's solution, and seawater. From this graph it can be observed that the corrosion resistance of Ti-6Al-4V in Ringer's solution is higher than in seawater and 3.5% NaCl. This is observed by the higher values of corrosion potential and lowest values of corrosion current.

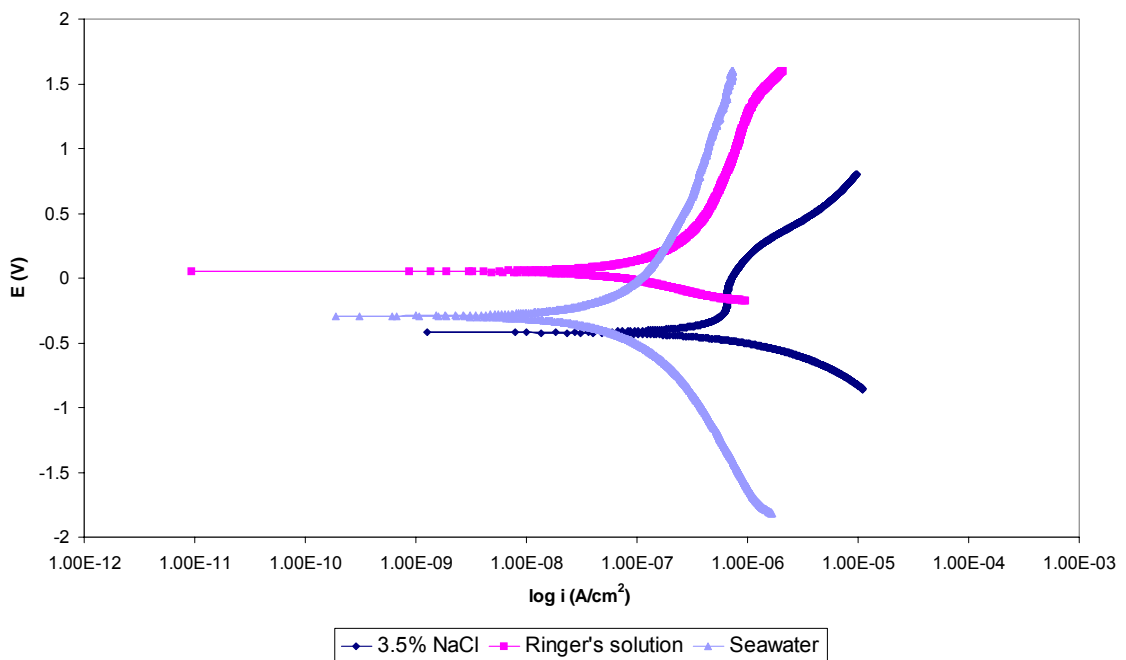


Figure 4-11. Potentiodynamic anodic polarization curves for Ti-6Al-4V after thermal treatment at 800°C

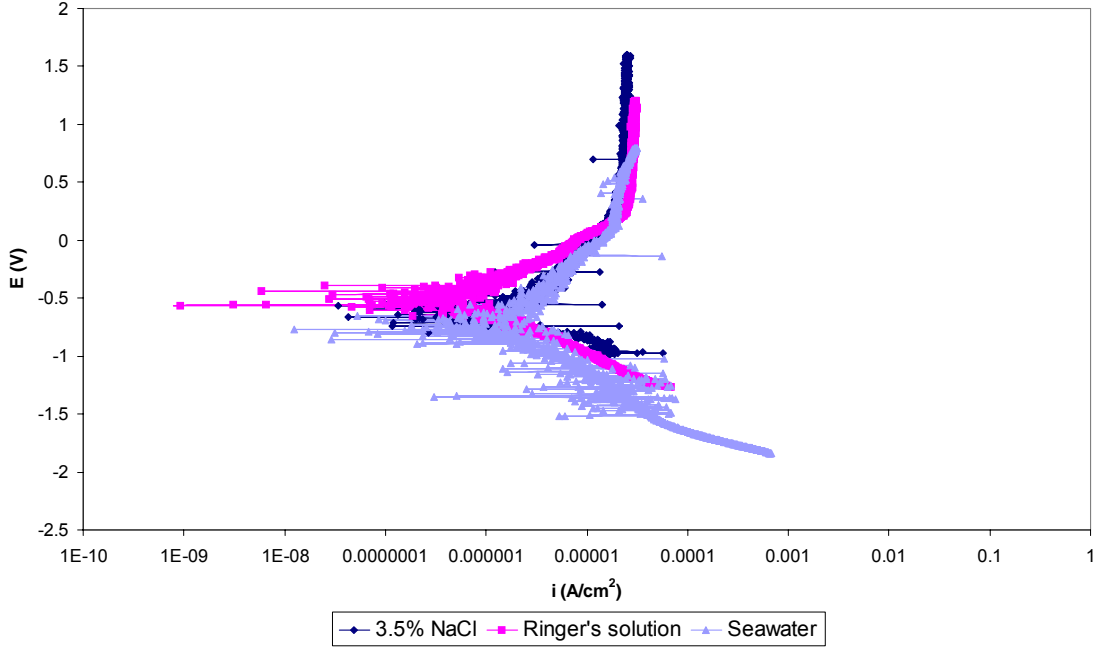


Figure 4-12. Potentiodynamic anodic polarization curves for Ti-6Al-4V control

Many studies about corrosion evaluation of Ti-6Al-4V have been carried out and a comparison with this study is essential. In a study made by Wen-Wei et al. [17], this alloy was evaluated in three biological solutions: urine, serum, and joint fluid. It was observed that the corrosion resistance of Ti-6Al-4V implant alloy in urine was higher than in the other electrolytes because the t_{corr} obtained in this medium was lowest at a range of 0.16-0.31 $\mu\text{A}/\text{cm}^2$ and the E_{corr} value was -0.180 V, the highest in comparison with the other media. Similar results are obtained in this research. Additionally, these authors report that in a previous evaluation of this alloy the corrosion current density of Ti-6Al-4V is high for values of the order of $45.93\mu\text{A}/\text{cm}^2$ in 0.6 N NaCl. To compare with the results obtained in the present work, the values found for this parameter were in a range of $1.94\text{-}8.24\mu\text{A}/\text{cm}^2$ and $0.14\text{-}3.52\mu\text{A}/\text{cm}^2$ for γ -TiAl and Ti-6Al-4V, respectively, values

well below those reported. In another study, Metikos et al [25], evaluated Ti-6Al-4V, along with Ti-6Al-6Nb, in Hank's solution and found a qualitatively similar behavior between these materials in a potential range from -1 to $4V$, but when the potential increased, Ti-6Al-4V experienced an anodic breakdown (oxide film rupture) at a potential of $4V$, while Ti-6Al-6Nb exhibited a steady current plateau that resisted the oxide film breakdown with no observed pitting up to $10V$. Even though in the present research the potential range is not sufficiently high to produce pitting corrosion in the alloy, the film breakdown of Ti-6Al-4V is one of the main characteristics that determine the possibility of vanadium ion release of this alloy, and one of the reasons that merit the search for alternative titanium alloys to be used as biomaterials.

In the present research the Ti-6Al-4V surface was modified with thermal treatment at $500^{\circ}C$ and $800^{\circ}C$ for 1 hr to improve its corrosion resistance. A protective titanium oxide layer, rutile, was formed with these treatments. The results show low values of C_R in comparison with the control samples. In a study made by Garcia-Alonso et al [9] Ti-6Al-4V was exposed to a thermal oxidation at $500^{\circ}C$ and $700^{\circ}C$ for the same time and was evaluated in Ringer's solution with anodic polarization tests. The results showed very low passive current density values for both treatments, which indicated the high corrosion resistance of this alloy. In another study, Cai et al [20] also evaluated Ti-6Al-4V, modifying its surface with three different treatments. For this purpose, they used the polarization resistance (R_p) technique and, as an electrolyte, they used a simulated oral environment (Zucchi synthetic saliva). The corrosion current i_{corr} of the alloy was determined according to the Stern-Geary equation [32] and the results showed

values lower than those found in the present work, in the nA/cm^2 range. These results were attributed to the formation of hydrated Ti (IV) oxide, a form of titanium oxide, and a stable Al (III) oxide obtained with superficial treatments. In comparison in the present research, only rutile was formed with the oxidation treatments. From these results it is important to note, that corrosion resistance of alloys is directly related to the surface condition before corrosion evaluation, and is the determining factor in the electrochemical behavior of these alloys.

4.2.1.1 Effect of medium temperature

To evaluate the temperature effect on the titanium alloys, control and autoclaved samples were tested in Ringer's solution at three different temperatures. It is well known that, if the electrolyte temperature increases, the corrosion resistance decreases due to increased diffusion of oxygen on the alloys. The present evaluation was not an exception. The medium temperature (Ringer's solution), was increased from 25°C to 30°C and 37°C (human body temperature) and the corrosion resistance of both alloys decreased, but not significantly. Tables 4.3 and 4.4 show the results found for control and autoclaving samples of γ -TiAl and Ti-6Al-4V, respectively. From these tables it can be seen that t_{corr} and C_R increased for 30°C and 37°C with respect to 25°C for both alloys. Yet, it is important to note that even though these values increased, they were still relatively low. Figures 4.13 and 4.14 are the polarizations curves obtained experimentally that confirm these results for control samples of γ -TiAl and Ti-6Al-4V, respectively. Figures 4.15 to 4.17 show this behavior, where the average values obtained for E_{corr} , I_{corr} , and C_R are a

function of the temperature. It can be observed that in these graphs, even though the corrosion resistance decreases as the temperature increases, the autoclaved samples for both alloys have a better corrosion resistance than the control samples. This is due to the presence of the protective layer formed with this treatment on the alloys.

Table 4-3. Corrosion parameters of γ -TiAl for temperature effect

MATERIAL	TREATMENT	ELECTROLYTE	β_a	β_c	E _{corr}	i _{corr}	C _R
			(mV/decade)	(mV/decade)	(V)	(μ A/cm ²)	(mm/y)
γ -TiAl	Control-25C	Ringer's solution	556.51 \pm 38.2	373.78 \pm 21.9	-0.615 \pm 0.083	2.56 \pm 0.73	4.40E-02 \pm 0.021
γ -TiAl	Control-30C	Ringer's solution	346.63 \pm 41.5	253.36 \pm 48.1	-0.639 \pm 0.043	0.43 \pm 0.34	2.06E-02 \pm 0.057
γ -TiAl	Control-37C	Ringer's solution	488.03 \pm 27.9	302.13 \pm 30.9	-0.735 \pm 0.038	5.86 \pm 0.41	5.58E-02 \pm 0.069
γ -TiAl	Autoclaving-25C	Ringer's solution	*	*	*	*	*
γ -TiAl	Autoclaving-30C	Ringer's solution	354.16 \pm 16.8	317.54 \pm 35.2	-0.276 \pm 0.041	0.14 \pm 0.37	6.75E-04 \pm 0.045
γ -TiAl	Autoclaving-37C	Ringer's solution	502.8 \pm 26.7	280.83 \pm 21.4	-0.455 \pm 0.052	0.44 \pm 0.31	1.04E-03 \pm 0.022

Table 4-4. Corrosion parameters of Ti-6Al-4V for temperature effect

MATERIAL	TREATMENT	ELECTROLYTE	β_a	β_c	E _{corr}	i _{corr}	C _R
			(mV/decade)	(mV/decade)	(V)	(μ A/cm ²)	(mm/y)
Ti-6Al-4V	Control-25C	Ringer's solution	356.89 \pm 28.9	270.04 \pm 32.3	-0.599 \pm 0.029	0.21 \pm 0.42	2.44E-03 \pm 0.042
Ti-6Al-4V	Control-30C	Ringer's solution	584.97 \pm 22.8	336.57 \pm 69.3	-0.626 \pm 0.031	2.52 \pm 0.18	2.97E-02 \pm 0.046
Ti-6Al-4V	Control-37C	Ringer's solution	882.57 \pm 38.1	599.53 \pm 37.9	-0.577 \pm 0.046	6.13 \pm 0.29	7.22E-02 \pm 0.028
Ti-6Al-4V	Autoclaving-25C	Ringer's solution	*	*	*	*	*
Ti-6Al-4V	Autoclaving-30C	Ringer's solution	636.54 \pm 49.4	342.78 \pm 28.6	-0.295 \pm 0.055	0.18 \pm 0.33	2.10E-03 \pm 0.039
Ti-6Al-4V	Autoclaving-37C	Ringer's solution	835.79 \pm 25.7	475.77 \pm 73.7	-0.428 \pm 0.038	0.59 \pm 0.28	8.66E-03 \pm 0.027

In a study made by Ionipa et al [27], Ti-5Al-4V alloy, a titanium alloy similar to Ti-6Al-4V was evaluated by linear polarization in Ringer's solution at 37°C and exposed for 12,000 hours. The results showed a good corrosion resistance for this alloy with increasing C_R in a range of 4.2*10⁻³ to 6.48*10⁻³ mm/y with increasing time. Even though, in the present work, increasing time of exposure was not one of the variables that were studied, the results found for Ti-6Al-4V were very similar to those found for autoclaved samples of γ -TiAl and Ti-6Al-4V in Ringer's solution at 37°C.

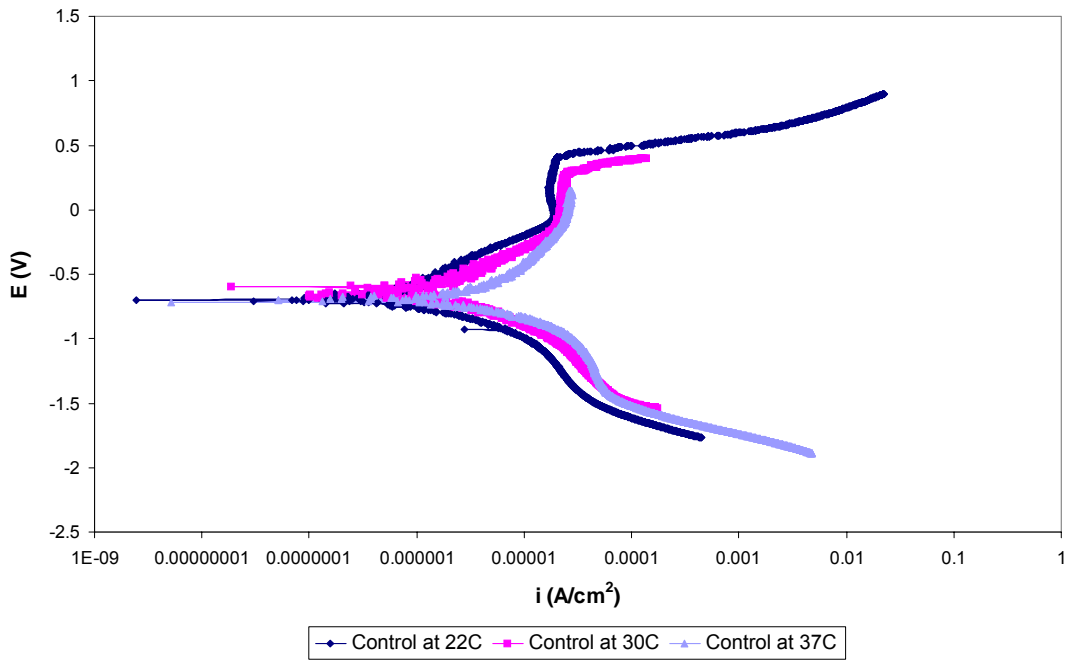


Figure 4-13. Temperature effect in control samples of γ -TiAl

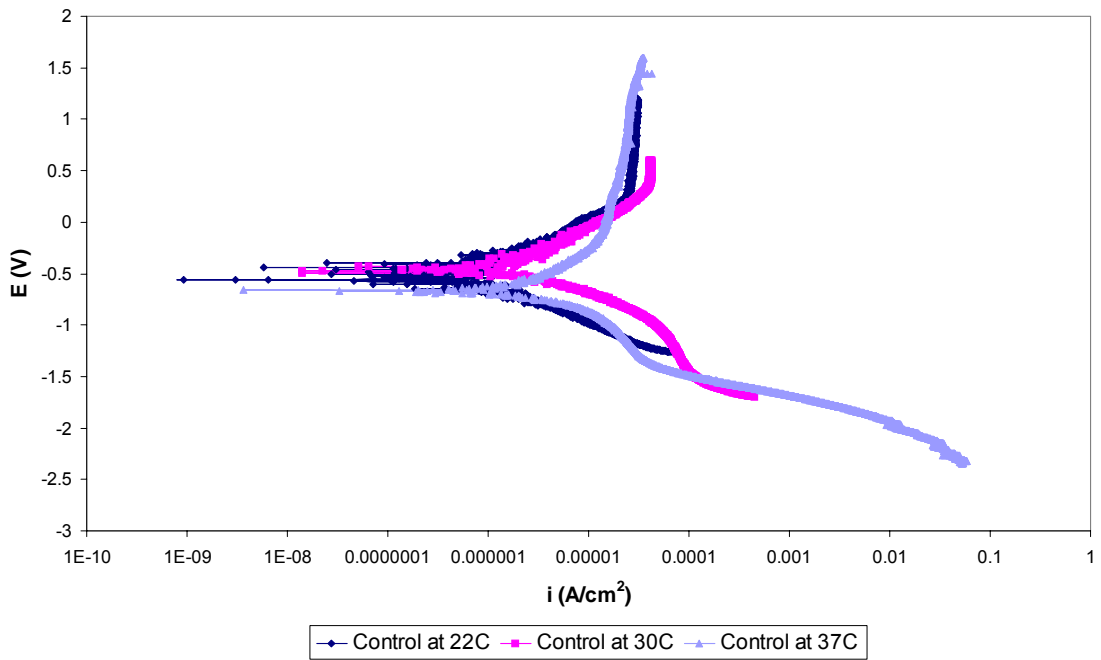


Figure 4-14. Temperature effect in control samples of Ti-6Al-4V

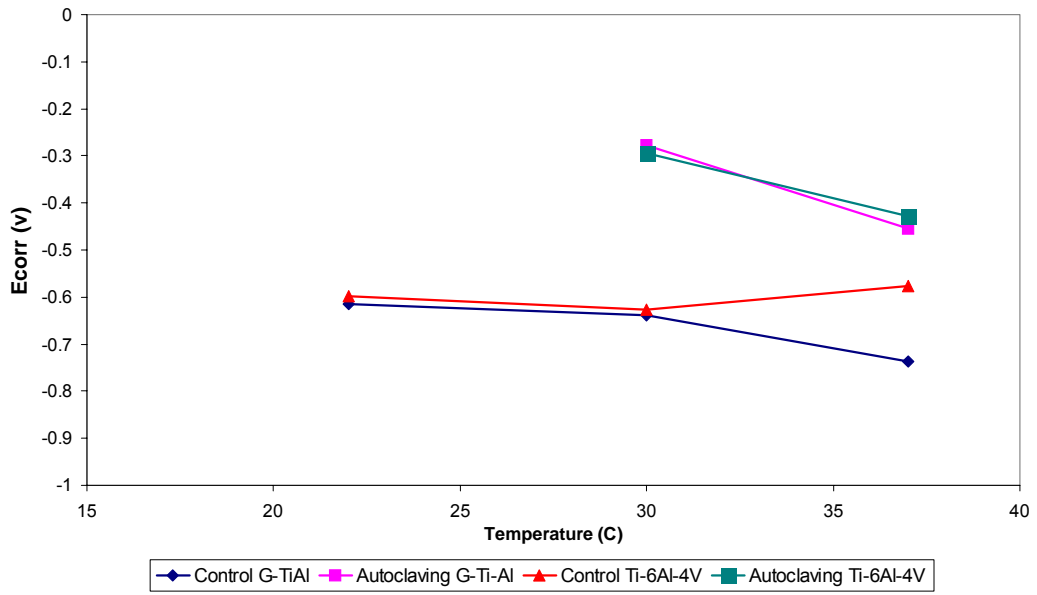


Figure 4-15. E_{corr} vs Temperature

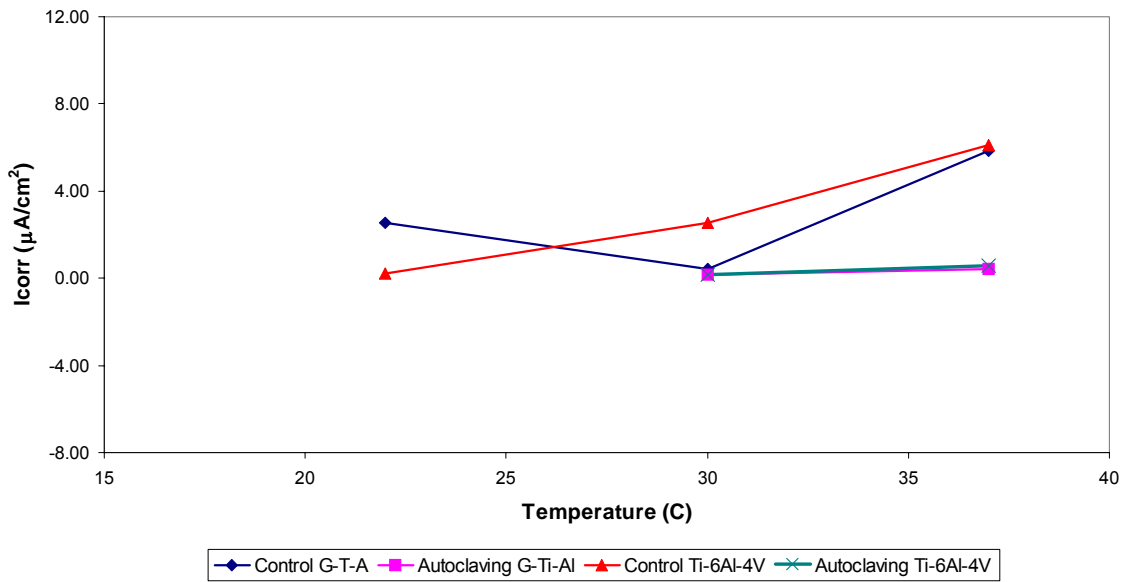


Figure 4-16. I_{corr} vs Temperature

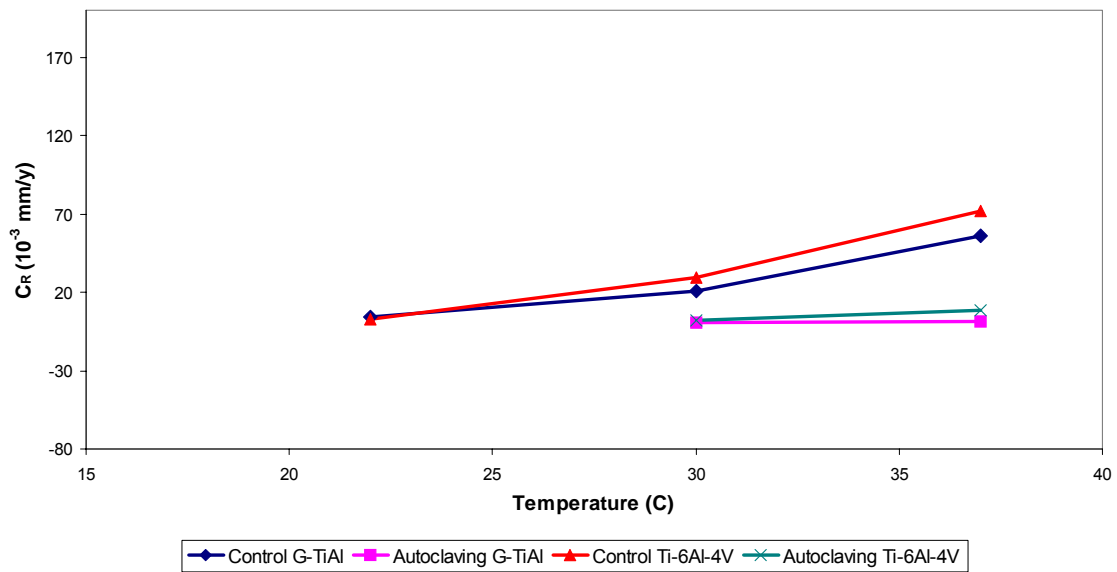


Figure 4-17. Corrosion rate vs Temperature

With the purpose of determining the relationship between corrosion rate (C_R) and temperature, the Arrhenius equation was used as a model to determine the activation energy (E_a). This parameter indicates the rate controlling mechanism of the process, which in this case corresponds to the corrosion resistance of titanium alloys. Table 4.5 shows the activation energy values calculated for control and autoclaved samples of γ -TiAl and Ti-6Al-4V and Figure 4.18 presents this behavior for both alloys in Ringer's solution.

Table 4-5. Activation energy values for control and autoclaved samples of γ -TiAl and Ti-6Al-4V

MATERIAL	TREATMENT	E_a (KJ/mol)
γ -TiAl	control	159.84
γ -TiAl	autoclaved	47.95
Ti-6Al-4V	control	210.39
Ti-6Al-4V	autoclaved	158.20

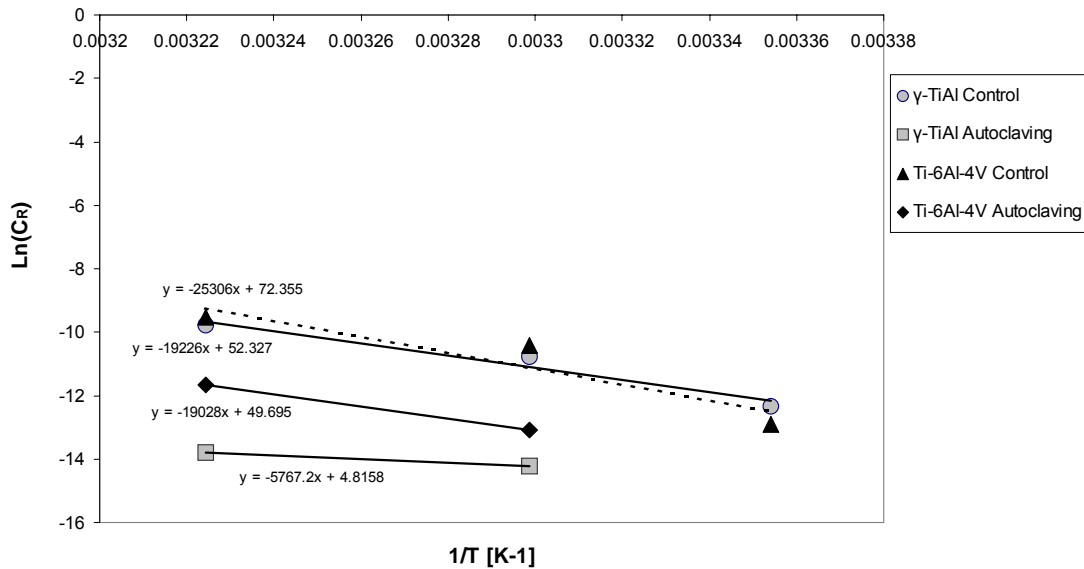


Figure 4-18. Arrhenius plot for γ -TiAl and Ti-6Al-4V control and autoclaved samples in Ringer's solution

4.2.2 Electrochemical impedance spectroscopy (EIS)

Electrochemical impedance spectroscopy is an ac technique used to evaluate the corrosion behavior of the two titanium alloys in this study. This technique was used to compare the results obtained from potentiodynamic anodic polarization tests. From this method, Nyquist plots and Bode plots were obtained and analyzed to determine the solution resistance (R_{Ω}), polarization resistance at the electrode/solution interface (R_p), and a double layer capacitance at this interface (C_{DL}). Among these parameters, R_p is the factor that determines corrosion resistance of alloys. This value is inversely proportional to t_{corr} , and hence, high values of R_p , correspond to low values of C_R .

Table 4.6 and Table 4.7 show the corrosion parameters obtained for γ -TiAl and Ti-6Al-4V with this technique. These tables show the values of electrolyte resistance (R_{Ω}), oxide layer resistance (R_{oxide}), polarization resistance (R_{film}), oxide layer frequency (W_{oxide}), and film frequency (W_{film}) obtained directly from the Nyquist plot, and the capacitance of the oxide layer (CPE_{oxide}) and film layer (CPE_{film}) calculated with a standard equation.

Table 4-6. Ac impedance parameters for γ -TiAl for all treatments

MATERIAL	TREATMENT	ELECTROLYTE	R_{Ω} ($\Omega.cm^2$)	R_{oxide} ($K\Omega.cm^2$)	R_{film} ($M\Omega.cm^2$)	W_{OXIDE} (Hz)	CPE_{OXIDE} ($\mu F/cm^2$)	W_{film} (mHz)	CPE_{film} ($\mu F/cm^2$)
γ -TiAl	Control	3.5 % NaCl	5.23 \pm 0.25		2.47 \pm 0.85			2.87 \pm 0.31	22.45 \pm 1.43
γ -TiAl	Control	Ringer's solution	10.61 \pm 1.31		0.42 \pm 0.79			6.39 \pm 0.53	60.64 \pm 4.78
γ -TiAl	Control	Seawater	1.49 \pm 0.52		0.11 \pm 0.65			47.12 \pm 2.45	30.08 \pm 3.51
γ -TiAl	Oxidation at 500C	3.5 % NaCl	5.23 \pm 0.36		1.03 \pm 0.91			39.8 \pm 1.98	3.89 \pm 1.12
γ -TiAl	Oxidation at 500C	Ringer's solution	27.3 \pm 2.18		23.92 \pm 2.75			3.14 \pm 0.98	2.12 \pm 0.98
γ -TiAl	Oxidation at 500C	Seawater	1.39 \pm 0.28		7.34 \pm 0.98			*	*
γ -TiAl	Oxidation at 800C	3.5 % NaCl	8.31 \pm 0.35	116.49 \pm 5.78	1.06 \pm 0.72	1.585 \pm 0.36	0.86 \pm 0.29	33.04 \pm 2.03	4.53 \pm 1.35
γ -TiAl	Oxidation at 800C	Ringer's solution	14.12 \pm 1.27	57.24 \pm 2.53	2.45 \pm 0.65	2.683 \pm 0.75	1.04 \pm 0.57	8.21 \pm 1.29	7.93 \pm 2.47
γ -TiAl	Oxidation at 800C	Seawater	1.71 \pm 0.33	*	0.04 \pm 0.81	*	*	*	*
γ -TiAl	Autoclaving	3.5 % NaCl	4.23 \pm 0.69		5.89 \pm 0.73			*	*
γ -TiAl	Autoclaving	Ringer's solution	8.53 \pm 0.46		9.02 \pm 1.88			1.52 \pm 0.85	11.6 \pm 2.38
γ -TiAl	Autoclaving	*	*		*	*	*	*	*

Table 4-7. Ac impedance parameters for Ti-6Al-4V for all treatments

MATERIAL	TREATMENT	ELECTROLYTE	R_{Ω} ($\Omega.cm^2$)	R_{oxide} ($K\Omega.cm^2$)	R_{film} ($M\Omega.cm^2$)	W_{OXIDE} (KHz)	CPE_{OXIDE} (nF/cm^2)	W_{film} (mHz)	CPE_{film} ($\mu F/cm^2$)
Ti-6Al-4V	Control	3.5 % NaCl	1.48 \pm 0.61		1.77 \pm 0.74			2.31 \pm 0.84	38.97 \pm 3.25
Ti-6Al-4V	Control	Ringer's solution	6.75 \pm 1.52		2.1 \pm 0.82			2.78 \pm 0.76	27.25 \pm 2.88
Ti-6Al-4V	Control	Seawater	1.14 \pm 0.47		0.17 \pm 0.76			13.9 \pm 2.05	69.24 \pm 4.67
Ti-6Al-4V	Oxidation at 500C	3.5 % NaCl	1.27 \pm 0.38		0.88 \pm 0.68			1.35 \pm 0.45	134.39 \pm 7.87
Ti-6Al-4V	Oxidation at 500C	Ringer's solution	5.48 \pm 1.16		0.65 \pm 0.53			1.0 \pm 0.49	245.33 \pm 38.71
Ti-6Al-4V	Oxidation at 500C	Seawater	1.28 \pm 0.49		2.23 \pm 0.95			*	*
Ti-6Al-4V	Oxidation at 800C	3.5 % NaCl	324.85 \pm 0.59	29.32 \pm 0.63	1.46 \pm 0.66	1.48 \pm 0.58	3.66 \pm 0.58	2.51 \pm 0.33	43.49 \pm 2.29
Ti-6Al-4V	Oxidation at 800C	Ringer's solution	98.85 \pm 0.34	5.25 \pm 0.58	1.72 \pm 0.93	4.25 \pm 1.92	7.13 \pm 2.79	1.93 \pm 1.04	47.89 \pm 3.17
Ti-6Al-4V	Oxidation at 800C	Seawater	393.87 \pm 0.29	188.59 \pm 3.31	1.93 \pm 0.74	2.41 \pm 0.42	0.35 \pm 0.23	35.13 \pm 4.26	2.35 \pm 1.25
Ti-6Al-4V	Autoclaving	3.5 % NaCl	5.2 \pm 0.57		5.24 \pm 0.80			1.0 \pm 0.77	30.39 \pm 3.85
Ti-6Al-4V	Autoclaving	Ringer's solution	5.95 \pm 0.33		11.14 \pm 2.85			1.35 \pm 0.93	10.61 \pm 2.98
Ti-6Al-4V	Autoclaving	*	*		*			*	*

The ac impedance parameters are directly related to the flow of electrons in an electrochemical system. For such reason these have, ideally, low values of electrolyte resistance (R_{Ω}) and high values of polarization resistance (R_{film}). If the R_{film} value is

higher, then the working electrode opposes changes from its equilibrium state, which corresponds to a low rate of titanium ion release and oxide growth. This behavior is clearly seen for γ -TiAl in Ringer's solution where these results were found. This behavior is in agreement with the results found with potentiodynamic anodic polarization (PAP). From Table 4.6 it can also be seen that, in general, for all treatments in the various electrolytes, there are high values of polarization resistance (R_{film}) in the order of mega-ohms ($M\Omega\cdot\text{cm}^2$), which implies a good corrosion resistance for this alloy. The passive film capacitance corresponds to the stability of the passive layer formed on the titanium alloys. For γ -TiAl, values in a range of 2.12 to 60.64 $\mu\text{F}/\text{cm}^2$ of CPE_{film} were found. Decreasing values correspond to a slow growth of the titanium oxide film, indicating a long-term stability of the passive layer. This behavior was observed for γ -TiAl, where the values decreased for the samples with surface treatments in comparison with control samples, where a passive layer was not formed. A similar behavior was found by Ionipa et al [27], where Ti-5Al-4V alloy was evaluated, and showed analogous results for resistance of the passive films and capacitance around 5 $M\Omega\cdot\text{cm}^2$ and 15 $\mu\text{F}/\text{cm}^2$, respectively.

Additionally, from Table 4.6, it is important to note that the results, obtained for samples oxidized at 800°C, present an additional R_{oxide} , $\text{CPE}_{\text{oxide}}$, and W_{oxide} parameters determined from the Nyquist plot. These values reveal the presence of an oxide layer formed with this surface treatment.

Table 4.7 shows the ac parameters obtained for Ti-6Al-4V. As in the case of γ -TiAl, the values obtained for R_{film} of Ti-6Al-4V were high, in the range of 0.17-11.14 $M\Omega.cm^2$; thus, indicating a good corrosion resistance for this alloy. In a study made by Metikos et al [31], R_{film} values, obtained experimentally for Ti-6Al-4V, were lower in comparison with the present work by $K\Omega.cm^2$. Comparing the results obtained for Ti-6Al-4V and γ -TiAl with respect to the behavior in Ringer's solution, the γ -TiAl alloy shows a better behavior due to the higher values of R_{film} in this medium. With respect to CPE_{film} values obtained for Ti-6Al-4V, these are higher in comparison with the results found for γ -TiAl, which means that there is a possibility of a more stable oxide layer formed. For Ti-6Al-4V samples oxidized at 800°C, the ac corrosion parameters correspond to the presence of a thick layer formed with this treatment. In a study made by Garcia et al. [9], the Ti-6Al-4V alloy was evaluated in an as-received condition, and thermally oxidized at 500°C and 700°C with EIS technique. The results obtained in this research were very similar with the results obtained in the present work. The R_{film} values found were in a range of 2.1 to 7.7 $M\Omega.cm^2$.

Impedance spectra, in Nyquist and Bode plots form, were obtained at open circuit potential. Figures 4.19 to 4.24 show some Nyquist plots obtained experimentally for the samples. Figure 4.19 show the comparison between the samples of γ -TiAl, evaluated in 3.5% NaCl. From this graph, it can be observed that autoclaved sample shows a better corrosion behavior in comparison with the other samples. This behavior can be attributed to the presence of a thin and continuous oxide layer formed on the alloy with this

treatment in comparison with the others treatments. Figures 4.20 and 4.21 show the Nyquist plot obtained for all samples of γ -TiAl in Ringer's solution and seawater, respectively. These impedance spectra show the best corrosion resistance for oxidized samples at 500°C in comparison with the other samples. This behavior can be attributed to the presence of a passive layer formed with this treatment, while for samples oxidized at 800°C the corrosion resistance was lower and can be explained due the presence of a discontinuous and porous oxide layer, which does not improve corrosion resistance for this alloy.

Figures 4.22 to 4.24 show the Nyquist plot obtained for Ti-6Al-4V in the different electrolytes. From these impedance spectra, it is important to note that the autoclaved samples showed a better behavior in comparison with the other treatments. From SEM micrographs (Figure 4.7) the presence of a thin oxide layer about 2 μ m thick on the Ti-6Al-4V surface was detected. The presence of this continuous layer improves the corrosion resistance of this alloy, manifested in the high values of R_{film} obtained experimentally.

From experimental results it is expected that similar values of electrolyte resistance (R_{Ω}) be measured regardless of modification of the working electrode. In the present research it was found that even though surface modifications were made on titanium alloys this parameter did not change significantly, giving grater credence to the experimental results.

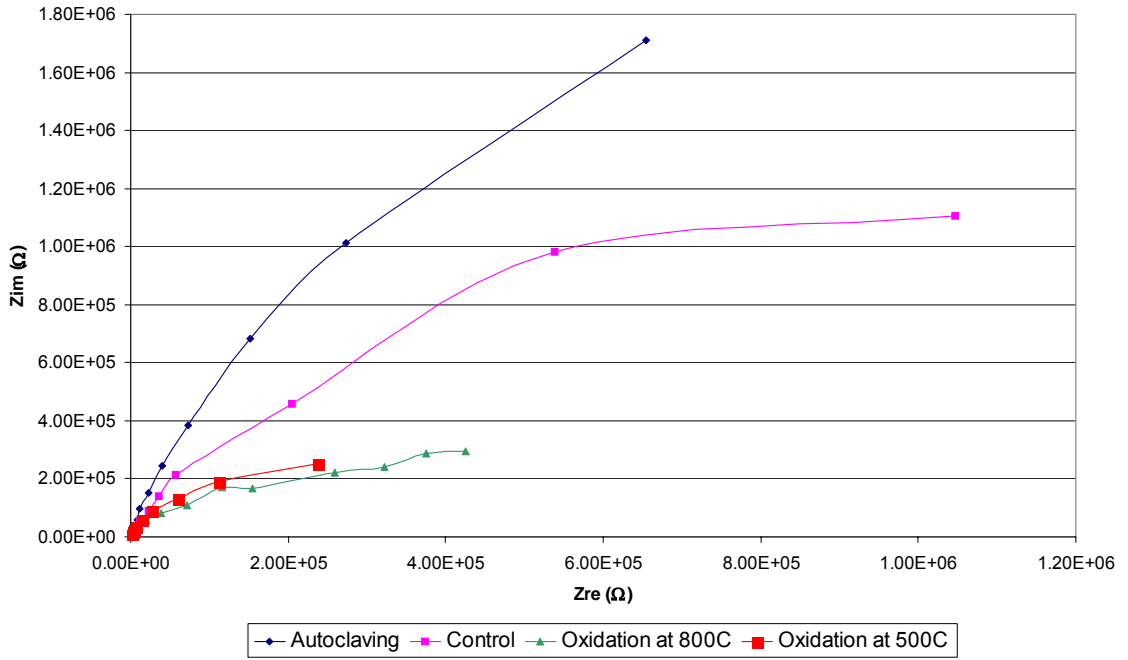


Figure 4-19. Nyquist plot for γ -TiAl in 3.5% NaCl

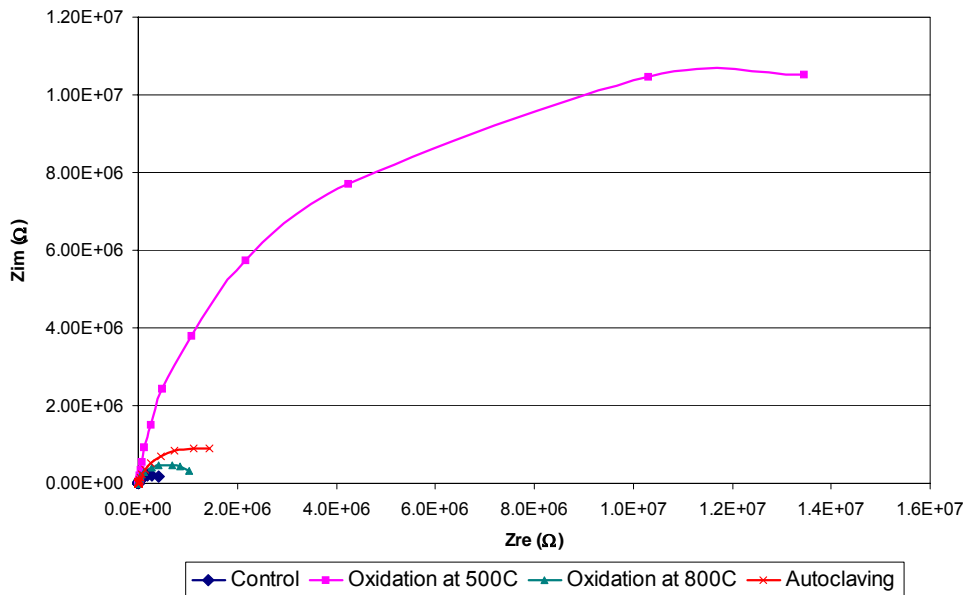


Figure 4-20. Nyquist plot for γ -TiAl in Ringer's solution

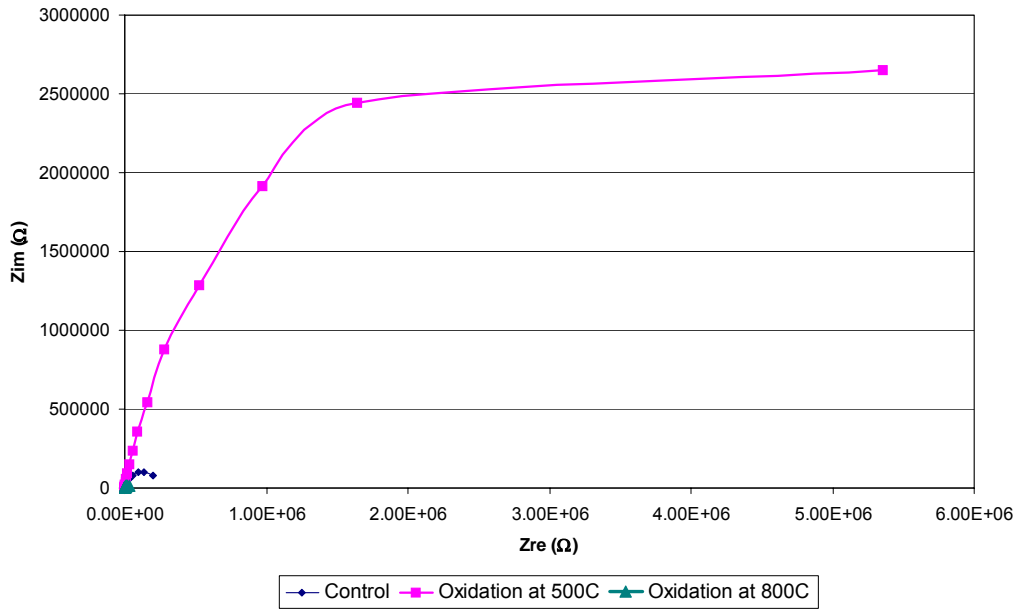


Figure 4-21. Nyquist plot for γ -TiAl in seawater

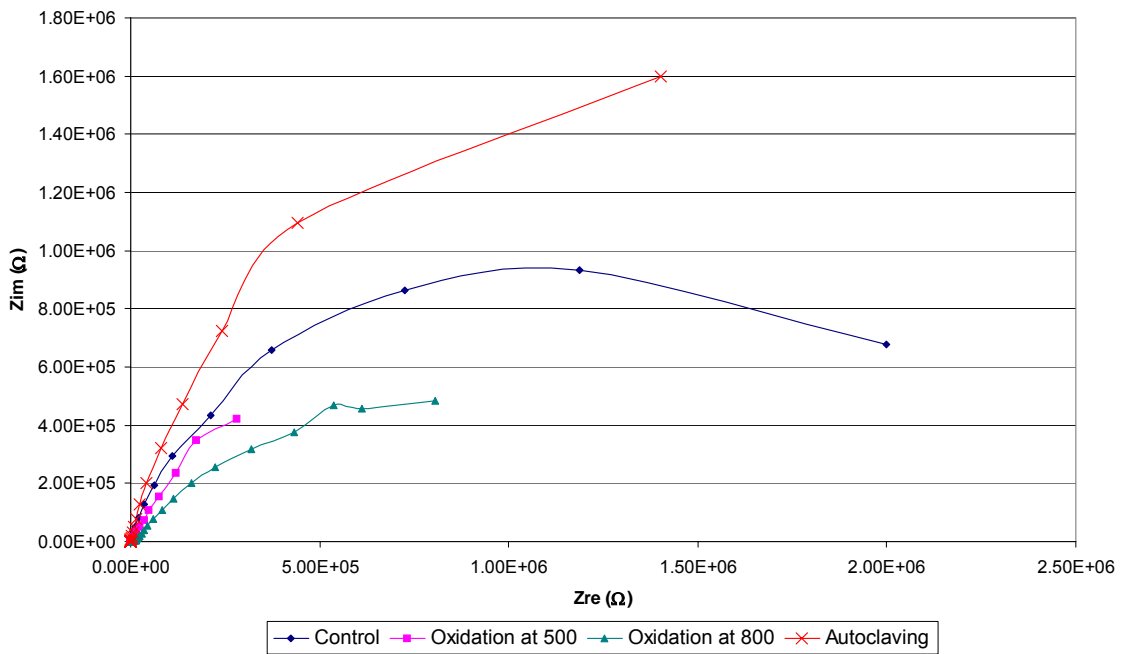


Figure 4-22. Nyquist plot for Ti-6Al-4V in 3.5% NaCl

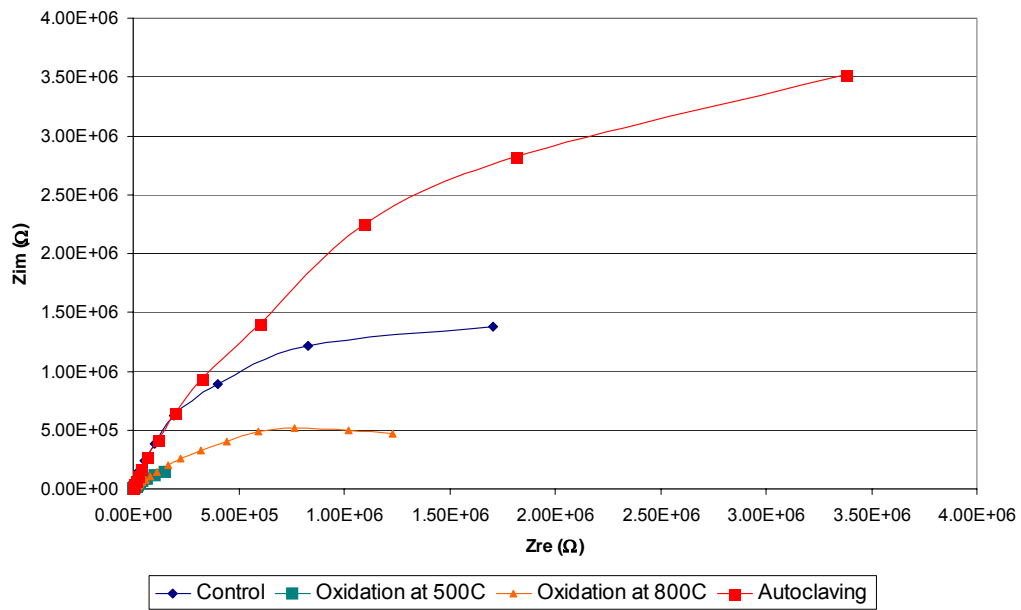


Figure 4-23. Nyquist plot for Ti-6Al-4V in Ringer's solution

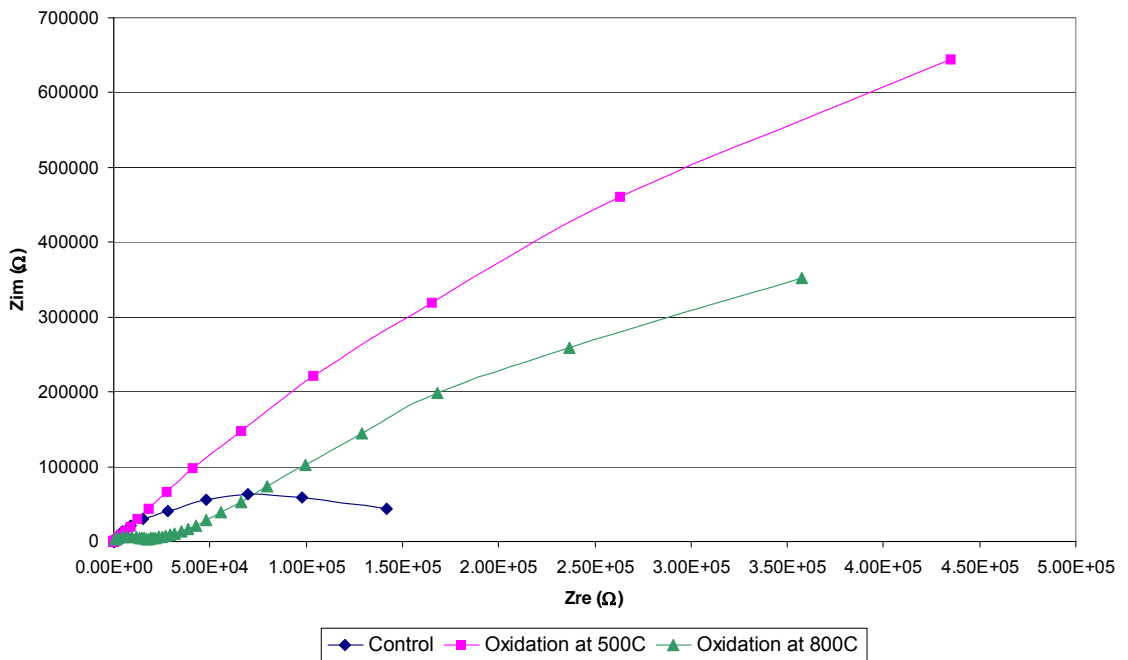
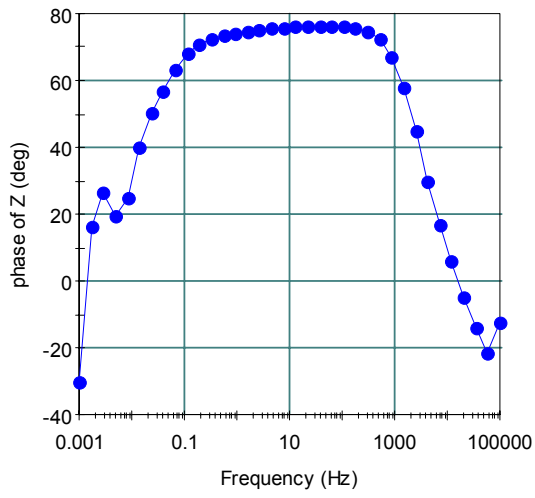


Figure 4-24. Nyquist plot for Ti-6Al-4V in seawater

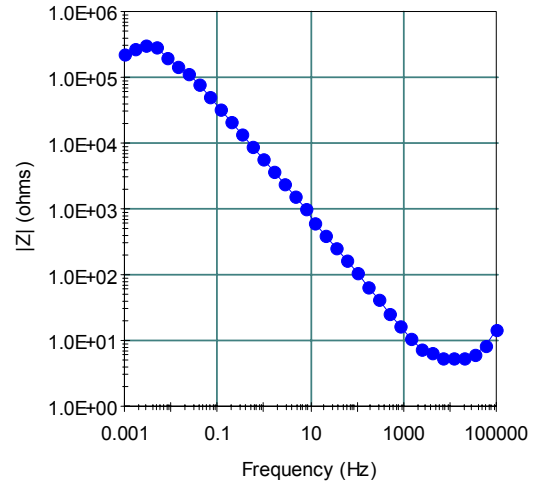
Bode plot spectra were evaluated to confirm the results obtained with Nyquist plots. Two different graphs were plotted: Bode Phase (Phase of Z Vs Frequency) and Bode $|Z|$ ($\log |Z|$ Vs Frequency). From these graphs it is possible to indicate the presence of a compact passive film, if: (a) the phase angle is close to -90° over a wide frequency range and (b) if the spectrum shows linear portions at intermediate frequencies, respectively.

For the three electrolytes, the impedance spectra found for γ -TiAl control exhibit a near capacitive response illustrated by a phase angle close to -80° , while the treated samples showed a phase angle close to -90° over a wide frequency range. This response corroborates the presence of a passive layer formed on this alloy with the surface treatment and the high values of R_p obtained from the Nyquist plot. Figure 4.25 shows representative Bode plots for γ -TiAl control samples in Ringer's solution, and Figure 4.26 shows representative Bode plots for γ -TiAl oxidized at 500°C . For Ti-6Al-4V, a similar behavior for control, autoclaved, and samples treated at 500°C was found but not for samples oxidized at 800°C . For these samples, the Bode Phase spectra show a decrease in phase angle at high frequencies from -80° to -15° and then a slight increase close to -40° . Additionally, the Bode $|Z|$ spectra indicates the deviation from the master line at intermediate frequencies. Figure 4.27 shows representative Bode plots for Ti-6Al-4V control in Ringer's solution and Figure 4.28 shows representative Bode plots for Ti-6Al-4V oxidized at 800°C . The behavior obtained for these samples is in agreement with the results achieved from the Nyquist plot; additional parameters (R_{oxide} , $\text{CPE}_{\text{oxide}}$, and W_{oxide}) were determined due to the presence of the oxide layer on this alloy,

the existence of a porous layer of rutile formed at 800°C was confirmed, and lower R_p values were determined in comparison with those obtained with the other surface treatments. A similar behavior was found by Garcia-Alonso et al. [9], where Ti-6Al-4V was oxidized at 500°C and 700°C; and the Bode $|Z|$ spectra also revealed a slight deviation from the master line for 700°C. They attributed this response to the presence of Al_2O_3 nuclei of lower resistance on the rutile scale that covered the surface of Ti-6Al-4V, which acts as easy diffusion paths through which the electric signal preferentially passes until reacting the substrate of this alloy, indicating a lower resistance and lower value of R_p in comparison with untreated samples as was observed in the present research. Wang et al. [43], found a similar response for untreated Ti-6Al-4V and, Ionipa et al. [27] obtained analogous results for Ti-5Al-4V. In general, a similar behavior was established for the three electrolytes for both titanium alloys.

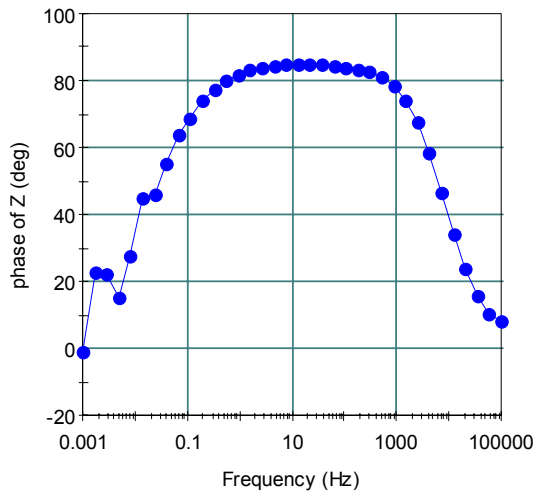


(a)

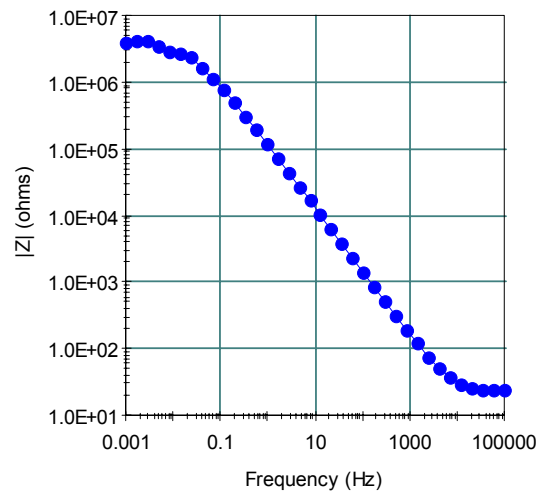


(b)

Figure 4-25. Bode Plots for γ -TiAl control in Ringer's solution (a) Bode Phase (b) Bode $|Z|$



(a)



(b)

Figure 4-26. Bode Plots for in Ringer's solution for γ -TiAl at 500°C (a) Bode Phase (b) Bode $|Z|$

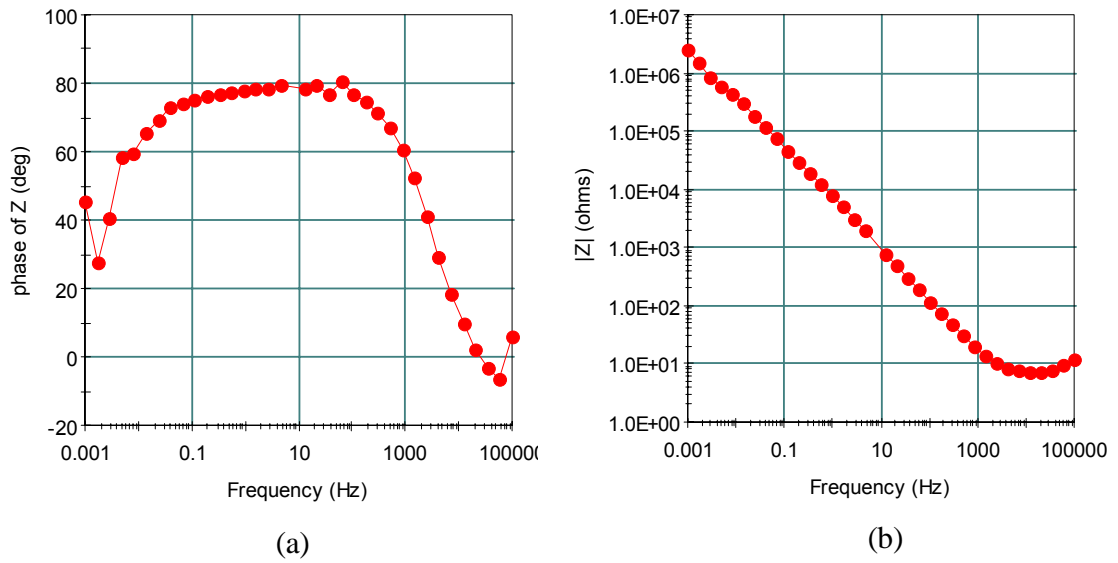


Figure 4-27. Bode Plots for Ti-6Al-4V control in Ringer's solution (a) Bode Phase (b) Bode $|Z|$

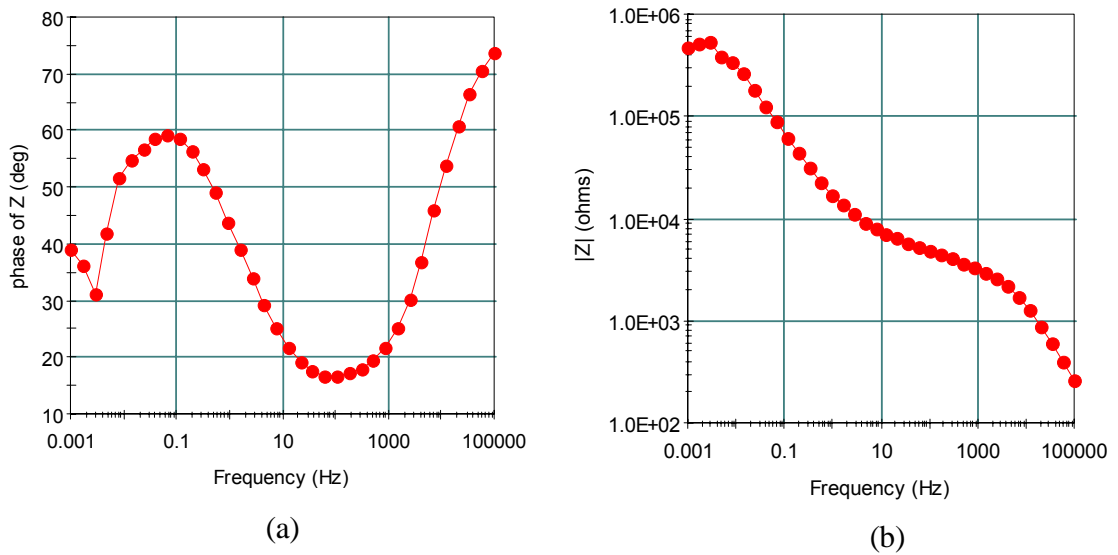


Figure 4-28. Bode Plots in Ringer's solution for Ti-6Al-4V oxidized at 800°C (a) Bode Phase (b) Bode $|Z|$

4.2.2.1 Equivalent circuit

An equivalent circuit model for corrosion behavior of the two titanium alloys being studied is proposed by simulating experimental impedance data. The circuits for ac model at the corrosion interface of both titanium implant alloys in the three electrolytes were based on Randles circuit.

The impedance data obtained for control and autoclaved samples and samples oxidized at 500°C for γ -TiAl and Ti-6Al-4V can be simulated by a simple RCPE couple, in which R_{Ω} is the electrolyte resistance, CPE_{film} corresponds to the double layer capacity and R_{film} is the polarization resistance at the electrode/solution interface. With respect to the data obtained for thermally treated samples at 800°C for both alloys, the electrochemical equivalent circuit that simulates the corrosion behavior of the oxidized samples is somewhat different from the other samples. In this case, a new box composed of CPE_{oxide} and R_{oxide} , is required to show the oxide layer formed with this treatment. Figure 4.29 shows the equivalent circuits proposed.

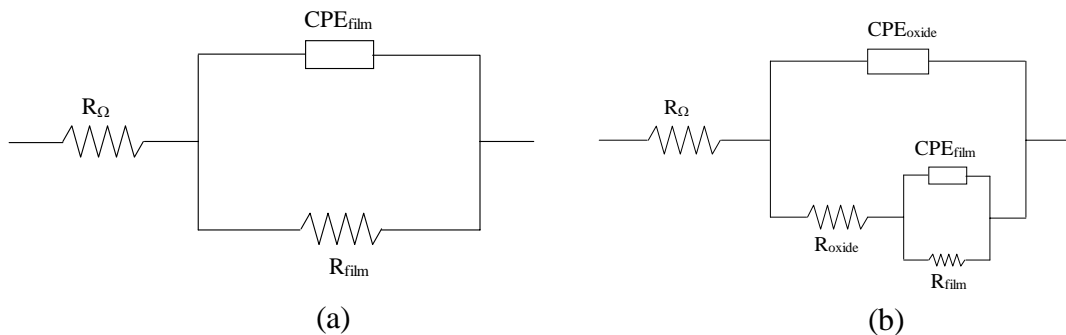


Figure 4-29. Equivalent electrochemical circuits for γ -TiAl and Ti-6Al-4V (a) simple RCPE for control, autoclaved, and oxidized at 500°C (b) RCPE for oxidation treatment at 800°C

4.2.2.2 Temperature effect evaluation

Table 4.8 and Table 4.9 present the ac impedance parameters obtained for control and autoclaved samples, at 25°C, 30°C, and 37°C, for γ -TiAl and Ti-6Al-4V, respectively. From both tables, it can be observed that when the temperature increases, the R_{film} decreases slightly. Even though this behavior represents a decrease in corrosion resistance for both alloys, the polarization resistance values are still high, in the order of mega-ohms ($M\Omega.cm^2$), indicating a good corrosion resistance for γ -TiAl and Ti-6Al-4V. A similar behavior was found with potentiodynamic anodic polarization technique where the C_R decreased when temperature increased. Figure 4.30 represents a summary of the behavior where the polarization resistance is a function of temperature.

Table 4-8. Ac impedance parameters for γ -TiAl for temperature effect

MATERIAL	TREATMENT	ELECTROLYTE	R_{Ω} ($\Omega.cm^2$)	R_{oxide} ($K\Omega.cm^2$)	R_{film} ($M\Omega.cm^2$)	W_{OXIDE} (Hz)	CPE_{OXIDE} ($\mu F/cm^2$)	W_{film} (mHz)	CPE_{film} ($\mu F/cm^2$)
γ -TiAl	Control-25C	Ringer's solution	10.61 \pm 1.31		0.42 \pm 0.79			6.39 \pm 0.53	60.64 \pm 4.78
γ -TiAl	Control-30C	Ringer's solution	7.05 \pm 0.48		0.61 \pm 0.65			6.53 \pm 1.24	40.3 \pm 2.92
γ -TiAl	Control-37C	Ringer's solution	6.02 \pm 0.27		0.18 \pm 0.33			18.71 \pm 2.86	46.91 \pm 3.15
γ -TiAl	Autoclaving-25C	Ringer's solution	8.53 \pm 0.46		9.02 \pm 1.88			1.52 \pm 0.85	11.6 \pm 2.38
γ -TiAl	Autoclaving-30C	Ringer's solution	8.34 \pm 0.36		2.54 \pm 0.76			2.47 \pm 1.05	25.32 \pm 2.87
γ -TiAl	Autoclaving-37C	Ringer's solution	4.57 \pm 0.22		1.58 \pm 0.55			1.69 \pm 0.92	59.38 \pm 4.23

Table 4-9. Ac impedance parameters for Ti-6Al-4V for temperature effect

MATERIAL	TREATMENT	ELECTROLYTE	R_{Ω} ($\Omega.cm^2$)	R_{oxide} ($K\Omega.cm^2$)	R_{film} ($M\Omega.cm^2$)	W_{OXIDE} (Hz)	CPE_{OXIDE} ($\mu F/cm^2$)	W_{film} (mHz)	CPE_{film} ($\mu F/cm^2$)
Ti-6Al-4V	Control-25C	Ringer's solution	6.75 \pm 0.52		2.1 \pm 0.82			2.78 \pm 0.76	27.25 \pm 2.88
Ti-6Al-4V	Control-30C	Ringer's solution	5.64 \pm 0.45		0.36 \pm 0.43			3.56 \pm 1.14	124.03 \pm 12.76
Ti-6Al-4V	Control-37C	Ringer's solution	6.58 \pm 0.17		0.32 \pm 0.29			6.43 \pm 1.88	77.38 \pm 3.29
Ti-6Al-4V	Autoclaving-25C	Ringer's solution	5.95 \pm 0.33		11.14 \pm 2.85			1.35 \pm 0.93	10.61 \pm 2.98
Ti-6Al-4V	Autoclaving-30C	Ringer's solution	6.45 \pm 0.39		0.76 \pm 0.44			3.93 \pm 0.96	53.11 \pm 5.78
Ti-6Al-4V	Autoclaving-37C	Ringer's solution	4.61 \pm 0.26		0.49 \pm 0.28			10.79 \pm 1.97	29.94 \pm 2.97

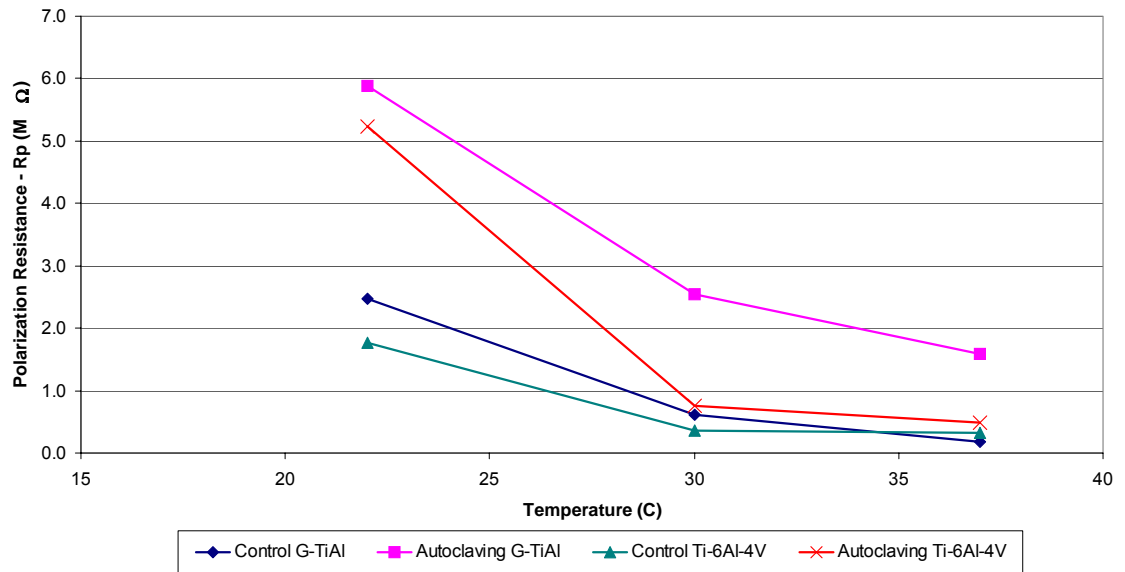


Figure 4-30. Temperature effect in control and autoclaved samples of γ -TiAl and Ti-6Al-4V with EIS technique

4.2.2.3 General results for γ -TiAl with EIS technique

Figure 4.31 summarizes the general behavior observed for γ -TiAl for all samples for all treatments. From this graph, it is important to note that the autoclaved samples and samples oxidized at 500°C show better corrosion resistance in Ringer's solution in comparison with the other treatments. From this result, it is possible to determine that any of these two surface treatments can be used to improve the corrosion resistance of γ -TiAl when the purpose is to employ this alloy as a biomaterial.

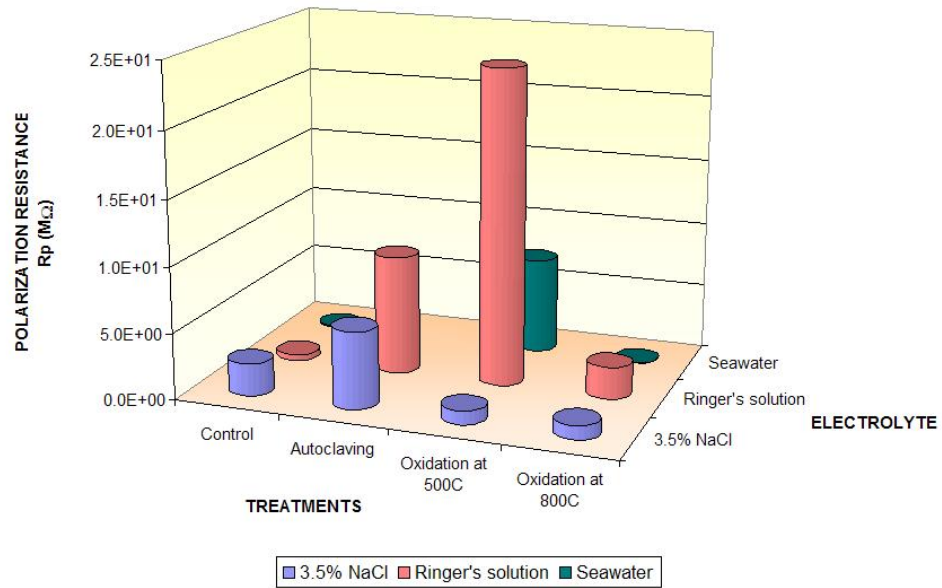


Figure 4-31. General behavior of γ -TiAl with EIS technique

4.2.2.4 General results for Ti-6Al-4V with EIS technique

Figure 4.32 summarizes the general behavior obtained for Ti-6Al-4V for all samples in all treatments. From this graph, it is important to note that autoclaved samples show a better behavior in comparison with the others samples. A similar behavior was obtained for γ -TiAl.

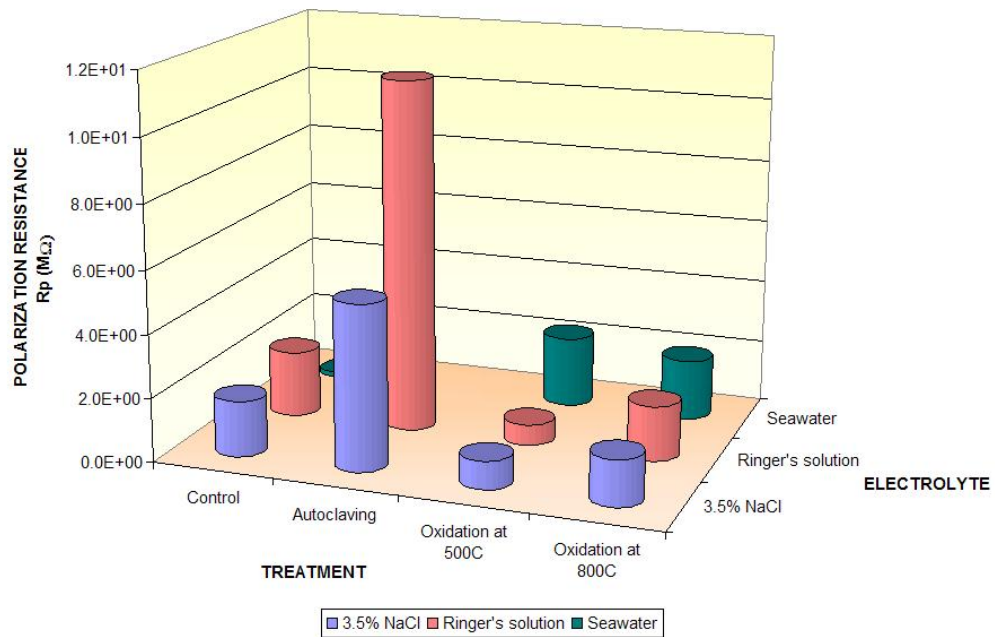


Figure 4-32. General behavior of Ti-6Al-4V with EIS technique

4.2.2.5 Comparison between γ -TiAl and Ti-6Al-4V with EIS technique

Figures 4.33, 4.34 and 4.35 present a compendium of the corrosion resistance of γ -TiAl and Ti-6Al-4V in 3.5% NaCl, Ringer's solution, and seawater, respectively. These graphs sum up the results mentioned above for the Nyquist plots in a comparative manner. From these graphs, it is important to note that, in general, γ -TiAl exhibits a resistance to corrosion as good as Ti-6Al-4V in terms of polarization resistance (R_{film}). In general, these are satisfactory results demonstrating that γ -TiAl shows an excellent corrosion resistance and it fulfills the requirements evaluated in this research to be considered as a possible biomaterial alloy.

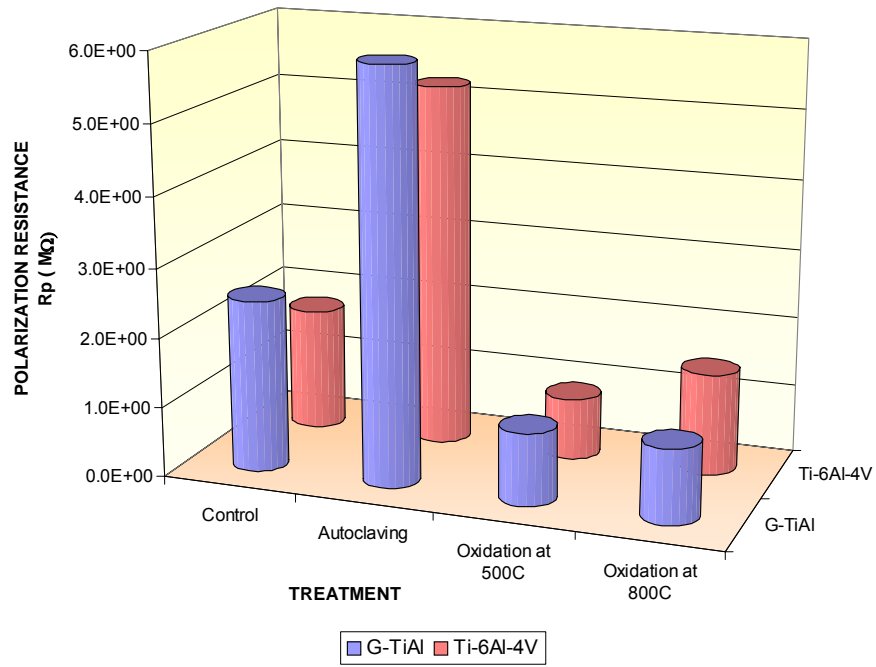


Figure 4-33. Behavior of γ -TiAl and Ti-6Al-4V in 3.5% NaCl

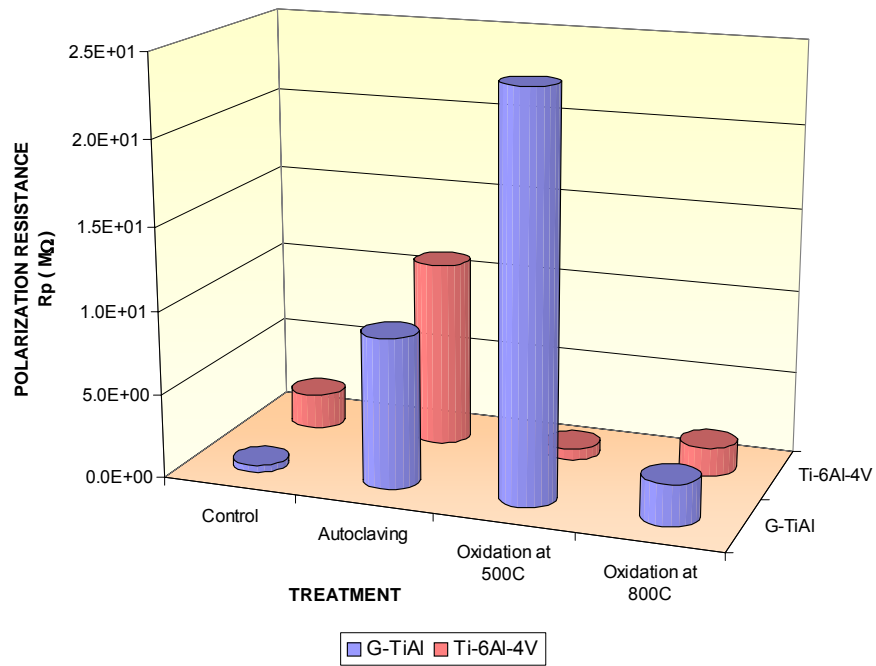


Figure 4-34. Behavior of γ -TiAl and Ti-6Al-4V in Ringer's solution

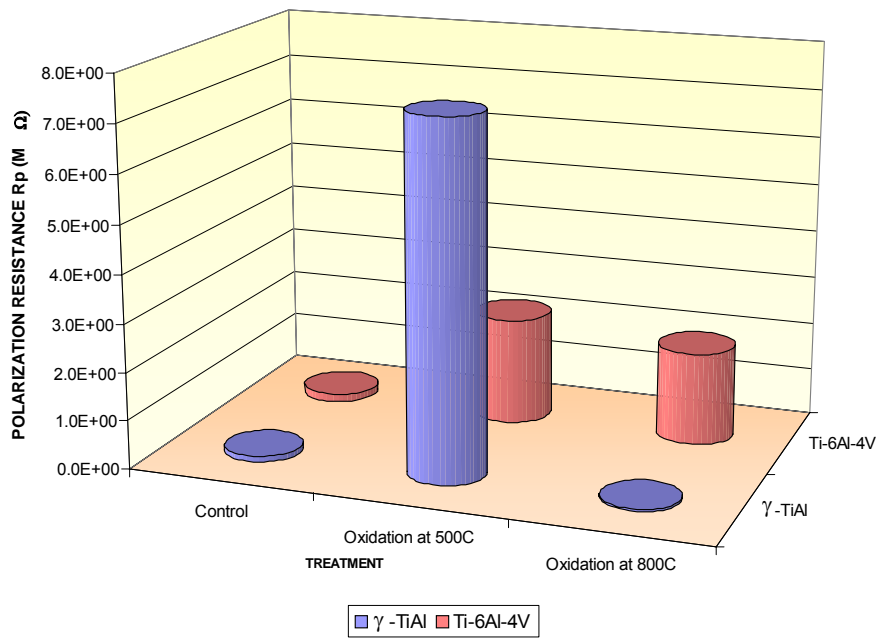


Figure 4-35. Behavior of γ -TiAl and Ti-6Al-4V in seawater

5 CONCLUSIONS

1. The kinetic parameters (β_a , β_c , E_{corr} , and t_{corr}) obtained by potentiodynamic anodic polarization technique were found in good agreement with that of EIS results.
2. The experimental results obtained with the two techniques show that γ -TiAl exhibits a similar corrosion behavior similar to Ti-6Al-4V.
3. The autoclaving process can be considered as an alternative surface treatment due to the formation of a more protective layer on the alloys manifested by increased corrosion resistance. This behavior was confirmed by the high values of polarization resistance (R_p) found using EIS.
4. Surface treatments are a good alternative to improve corrosion resistance of γ -TiAl and Ti-6Al-4V because they promotes the formation of an oxide layer on the surface.
5. The experimental results obtained to evaluate γ -TiAl with EIS and PAP in Ringer's solution show low values of corrosion rate (C_R) and high values of polarization resistance (R_p), parameters that are synonymous with excellent corrosion resistance required for biomaterial applications.
6. The electrochemical results obtained for γ -TiAl in 3.5% NaCl and seawater, in general, show a good corrosion behavior, a desirable response of this alloy in two aggressive media utilized as comparison to Ringer's solution electrolyte.
7. Even though corrosion rate (C_R) and polarization resistance (R_p) decrease when the temperature increases, this change is not significant since the values obtained are considered low and acceptable in applications where 37°C is the temperature

required, such as in biomaterials applications. Additionally, the behavior of the autoclaved samples, for both alloys, had a better corrosion resistance than control samples due to the presence of the protective layer formed with this treatment on the alloys.

8. In general, the low values for corrosion rate (C_R), and the high values for corrosion potential (E_{corr}) and Polarization resistance (R_p) obtained experimentally for γ -TiAl implies the possibility that it can be competitively considered as an alternative metallic biomaterial.

6 RECOMMENDATIONS

- ✓ As EIS permits in-situ characterization of passive films, evaluation of titanium alloys at different potentials and different exposure times to electrolytes can indicate the growth and stability of an oxide layer on the alloys, which increases the alloy's corrosion resistance.
- ✓ Study the mechanism of interaction between material and electrolyte.
- ✓ Increasing the exposure time of the samples in surface treatments, with the purpose of forming a thicker and continuous layer, would increase the corrosion resistance of these alloys.
- ✓ Increasing the frequency range in Electrochemical Impedance Spectroscopy technique will confirm the impedance parameters calculated by fitting.
- ✓ The transmission electron microscope (TEM) can be an alternative tool to characterize, in greater detail, the passive layer formed with the superficial treatments.

7 BIBLIOGRAPHY

- [1] Silver, F.H., Christiansen, D.L., *Biomaterials Science and Biocompatibility*. Springer, New York. 1999, pp 87-117
- [2] Black, J. *Biological Performance of Materials-Fundamentals of Biocompatibility*. 3rd Ed. Marcel Decker, Inc. New York. 1999, pp 119-128
- [3] Azom.com. “Titanium Alloys in Medical Applications” (online), The Titanium Information Group. 2/2004. www.azom.com/details.asp?ArticleID=1794
- [4] Azom.com. “Titanium and Titanium Alloys as Biomaterials” (online), The Titanium Information Group. 2/2004. www.azom.com/details.asp?ArticleID=1520
- [5] Black, J. “Does Corrosion Matter?”. *J Bone and Jt Surg*. Nov. 1988; 70B. pp.517-520
- [6] Wapner, K.L. “Implications of Metallic Corrosion in Total Knee Arthroplasty”. *Clin Orthop*. Feb 1991. 271 pp. 12-20
- [7] Castañeda, D.F. Evaluation of Gamma-TiAl as an Implant Material. M.S Thesis University of Puerto Rico, Mayaguez (2003)
- [8] Electrochemical Instruments Division. “Electrochemistry and Corrosion Overview and Techniques”. Princeton Applied Research. Application note corr-4.
- [9] Garcia-Alonso M.C., Saldaña L., Vallés G., González-Carrasco J.L., Gonzalez-Cabrero H., Martínez M.E., Gil-Garay E., Munuera L. “In Vitro Corrosion Behavior and Osteoblast Response of Thermally Oxidised Ti-6Al-4V Alloy”. *Biomaterials* 24. 2003, pp. 19-26
- [10] Davis J. R. *Handbook of Materials for Medical Devices*. ASM International. March 2004. p. 3
- [11] Solar, R.I., Pollack, S.R., Korostoff E. “In Vitro Corrosion Testing of Titanium Surgical Implant Alloy: an Approach to Understand Titanium Release from Implants”. *J.Biomed. Mater Res*. 1979, pp. 213-217
- [12] Milosev, I., Metikos-Hukovic M., Strehblow, H. “Passive Film on Orthopaedic TiAlV Alloy Formed in Physiological Solution Investigated by X-ray Photoelectron Spectroscopy”. *Biomaterials* 21. 2000. pp. 2103-2113.

- [13] Hodgson, A.W.E., Mueller, Y. "Electrochemical Characterization of Passive Films on Ti Alloys Under Simulated Biological Conditions". *Electrochimica Acta* 47. 2002. pp. 1913-1923.
- [14] Lopez, M. F., Gutierrez, A., Jimenez, J.A., "In Vitro Corrosion Behavior of Titanium Alloys without Vanadium". *Electrochimica Acta* 47. 2002. pp.1359-1364.
- [15] Khan, M. A., Williams, R.L. "The Corrosion Behavior of Ti-6Al-4V, Ti-6Al-7Nb and Ti-13Nb-13Zr in Protein Solutions". *Biomaterials* 20. 1999. pp. 631-637
- [16] Xia, J., Li, X.Y., et al. "The Structural and Mechanical Property Characterisation of Thermal Oxidation Treated γ -based Titanium Aluminide". *Thin Solid Films* 458. 2004. pp. 212-222.
- [17] Wen-Wei, R. H., Yang, C. C., Huang C.A., Chen Y. "Electrochemical Corrosion Properties of Ti-6Al-4V Implant Alloy in the Biological Environment". *Materials Science and Engineering A* 380. 2004, pp. 100-109.
- [18] Marciniak, J., Chrzanowski, W., Nawrat, G., Zak, J., Rajchel, B. "Structure Modification of Surface Layers of Ti-6Al-4V ELI implants". *Bioceramics*
- [19] Mizutani, M., Komotori, J., Katahira, K., Watanabe, Y., Ohmori, H. "Improvement of Corrosion Resistance and Mechanical Properties of the Biomaterial Ti-6Al-4V Alloy by ELID grinding". *Advances in Abrasive Technology VI*. 0-87849-933-4
- [20] Cai, Z., Ty, Shafer, Watanabe I., Nunn M., Okabe. T. "Electrochemical Characterization of Cast Titanium Alloys". *Biomaterials* 24. 2003. pp. 213-218.
- [21] Gurappa, I. "Protection of Titanium Alloy Components Against High Temperature Corrosion". *Materials Science and Engineering A356*. 2003. pp. 372-380.
- [22] Guleryuz, H., Cimenoglu, H. "Effect of Thermal Oxidation on Corrosion and Corrosion-wear Behaviour of a Ti-6Al-4V Alloy". *Biomaterials* 25. 2004. pp. 3325-3333.
- [23] Thierry, B., Tabrizian, M., Savadogo, O., Yahia, L.H. "Effects of Sterilization Processes on NiTi Alloy: Surface Characterization". *Journal of Biomedical Materials Research*. Vol. 49. No. 1, pp. 88-98 (2000)
- [24] Starosvetsky, D., Gotman, I. "Corrosion Behavior of Titanium Nitride Coated Ni-Ti Shape Memory Surgical Alloy". *Biomaterials* 22. 2001. pp. 1853-1859.

- [25] Metikos-Hukovic, M., Kwokal, A. "The Influence of Niobium and Vanadium on Passivity of Titanium-based Implants in Physiological Solution". *Biomaterials* 24. 2003. pp. 3765-3775.
- [26] Yong-Jae, Yu, Jung-Gu, Kim. "Localized Corrosion Behavior of Al₃Ti-Cr Alloys in 3.5 wt.% NaCl Solution". *Materials Science and Engineering A332*. 2002. pp. 140-145.
- [27] Ionipa, D., Santana-Lopez, A. "Electrochemical Impedance Spectroscopy Technique in Prediction of the Implant Titanium Alloys Behaviour". *European Cells and Materials*. Vol. 5. Suppl. 1, 2003. pp. 12-14.
- [28] Her-Hsiung, Huang. "In Situ Surface Electrochemical Characterizations of Ti and Ti-6Al-4V Alloy Cultured with Osteoblast-like Cells". *Biochemical and Biophysical Research Communications* 314. 2004. pp. 787-792.
- [29] Zeng, C.L, Zhang, T., "Electrochemical Impedance Study of Corrosion of B-1900 Alloy in the Presence of a Solid Na₂SO₄ and a Liquid 25 wt.% NaCl-75 wt.% Na₂SO₄ Film at 800°C in Air". *Electrochimica Acta* 49. 2004. pp. 1429-1433.
- [30] Perez, N. *Electrochemistry and Corrosion Science*. University of Puerto Rico. Mayaguez. 2003. pp. 89-93
- [31] Metikos, M., Kwokal, A "The Influence of Niobium and Vanadium on Passivity of Titanium-based Implants in Physiological Solution". *Biomaterials* 24. 2003. pp. 3765-3775.
- [32] Stearn, M., Geary, A. "Electrochemical polarization. I. A theoretical analysis of the shape of polarization curves". *J Electrochem Soc*. 1957. pp. 56-63
- [33] Sun, E.X., Nowak, W. B.. "Electrochemical Characteristics of Ti-6Al-4V Alloy in 0.2 N NaCl Solution I. Tafel Slopes in Quasi-passive State". *Corrosion Science* 43. 2001. pp. 1801-1816.
- [34] Yu, Y. J., Kim, J. G. "Localized Corrosion Behavior of Al₃Ti-Cr Alloys in 3.5 wt% NaCl Solution". *Materials science and engineering A332*. 2002. pp. 140-145.
- [35] Balajaru, J. N., Sankara-Narayanan, T.S.N. "Evaluation of the Corrosion Resistance of Electroless Ni-P and Ni-P Composite Coatings by Electrochemical Impedance Spectroscopy". *J Solid State Electrochem*. 2001. pp. 334-338.

- [36] Codaro, E.N., Nakazato, R.Z. "An Image Processing Method for Morphology Characterization and Pitting Corrosion Evaluation". *Materials Science and Engineering A334*. 2002. pp. 298-306.
- [37] Botella Ph., Frayret C. "Experimental Study, Via Current-potential Curves, of the Anodic Behavior of Alloy C-276 and T60 Titanium in Chlorinated and Oxygenated aqueous Media Under Sub- to Supercritical Conditions". *J. of Supercritical Fluids* 25. 2003. pp. 269-278.
- [38] Darowicki, K., Slepiski, P. "Instantaneous Electrochemical Impedance Spectroscopy of Electrode Reactions". *Electrochimica Acta* 49. 2004. pp. 763-772.
- [39] Donchev, A., Gleeson, B., et al. "Thermodynamic Considerations of the Beneficial Effect of Halogens on the Oxidation Resistance of TiAl-based Alloys". *Intermetallics* 11. 2003. pp. 387-398.
- [40] Xiaolong, Z., Chen J., Scheideler L., Reichl R., Geis-Gerstorfer J. "Effects of Topography and Composition of Titanium Surface Oxides on Osteoblast Responses". *Biomaterials* 25. 2004. pp. 4087-4103.
- [41] Hostis V.L., Dagbert C., Fe'ron D. "Electrochemical Behavior of Metallic Materials Used in Seawater-Interactions Between Glucose Oxidase and Passive Layers". *Electrochimica Acta* 48. 2003. pp. 1451-1458.
- [42] Tan, L., Bauer, J., et al "Biocompatibility Improvement of NiTi with a Functionally Graded Surface". *Society for Experimental Mechanics, 2002 SEM Annual Conference Proceedings, Milwaukee, WI, 2002*.
- [43] Wang, C.X., Wang, M. "Nucleation and Growth of Apatite on Chemically Treated Titanium Alloy: An Electrochemical Impedance Spectroscopy Study". *Biomaterials* 24. 2003. pp. 3069-3077.
- [44] Godfrey, A. Hu, D. "Properties and Microstructure of TiAl-based Alloys". *Materials Science and Engineering A239-240*. 1997. pp. 559-563.
- [45] Fergus, J.W. "Review of the Effect of Alloy Composition on the Growth Rates of Scales Formed During Oxidation of Gamma Titanium Aluminide Alloys". *Materials Science and Engineering A338*. 2002. pp. 108-125.

- [46] Popa, M.V., Demetrescu, I., Valisescu E., Drob P., Lopez A., Mirza-Rosca J., Vasilescu C., Ionita D. "Corrosion Susceptibility of Implant Materials Ti-5Al-4V and Ti-6Al-4Fe in Artificial Extra-cellular Fluids". *Electrochimica Acta* 49. 2004. pp. 2113-2121.
- [47] Hsu, R.W., Yang, C.C. "Electrochemical Corrosion Properties of Ti-6Al-4V Implant Alloy in the Biological Environment". *Materials Science and Engineering A* 380. 2004. pp. 100-109.
- [48] Chaoliu, Z., Pingyi, G., Weitao W. "Electrochemical Impedance of Two-phase Ni-Ti Alloys During Corrosion in Eutectic $(0.62\text{Li},0.38\text{K})_2\text{CO}_3$ at 650°C ". *Electrochimica Acta* 49. 2004. pp. 2271-2277.